

# First high-nuclearity palladium halide/carbonyl/phosphine cluster, $[\text{Pd}_{12}(\mu_3\text{-I})_2(\mu_4\text{-I})_3(\mu_2\text{-CO})_6(\text{PEt}_3)_6]^+$ monocation containing an octacapped octahedral $\text{Pd}_6(\mu_3\text{-Pd})_6(\mu_3\text{-I})_2$ fragment: structure-to-synthesis generation from different synthetic routes

Evgueni G. Mednikov, Lawrence F. Dahl \*

*Department of Chemistry, University of Wisconsin-Madison, Madison, WI 53706, USA*

Received 9 August 2004; accepted 1 September 2004

Available online 4 February 2005

Dedicated to Gordon Stone, a highly creative and exceptionally prolific inorganic chemist, for his many outstanding accomplishments and leadership in organometallic chemistry during his illustrious scientific career over approximately 50 years at Harvard University, Queen Mary College (University of London), University of Bristol, and Baylor University

## Abstract

The original synthesis and stereochemical characterization of the  $[\text{Pd}_{12}(\mu_3\text{-I})_2(\mu_4\text{-I})_3(\mu_2\text{-CO})_6\text{L}_6]^+$  monocation (**1**) ( $\text{L} = \text{PEt}_3$ ;  $[\text{PF}_6]^-$  salt) was an outgrowth of our investigation of the chemical behavior of two unusual thallium–palladium clusters:  $(\mu_6\text{-Tl})[\text{Pd}_3(\text{CO})_3\text{L}_3]_2^+$  (**2**) which possesses a  $\text{Pd}_3\text{TlPd}_3$  sandwich framework, and  $[\text{Tl}_2\text{Pd}_{12}(\text{CO})_9\text{L}_9]^{2+}$  (**3**) which may be viewed as edge-fusions of three  $\text{Pd}_3$  trigonal bipyramids to a central  $\text{Tl}_2\text{Pd}_3$  trigonal bipyramid. Room-temperature reactions of **2** and **3** with  $\text{I}_2$  in THF gave rise in each case to small yields (<10%) of **1** along with two square-planar palladium(II) co-products, *trans*- $\text{Pd}_2(\mu_2\text{-I})_2\text{I}_2\text{L}_2$  (**7**) and *trans*- $\text{PdI}_2\text{L}_2$  (**8**) ( $\text{L} = \text{PEt}_3$ ). The geometries and compositions of **1**, **7**, and **8** were unequivocally established from low-temperature CCD X-ray crystallographic determinations. **1** was characterized by solid-state/solution IR and multinuclear ( $^{31}\text{P}$ ,  $^{13}\text{C}$ ,  $^1\text{H}$ ) NMR spectra. The 12-atom metal-core architecture of this geometrically unprecedented  $\text{Pd}_6(\mu_3\text{-Pd})_6(\mu_3\text{-I})_2(\mu_4\text{-I})_3$  kernel of **1** of crystallographic  $D_3$  (32) site symmetry may be envisioned as a distorted hexacapped octahedral  $\text{Pd}(\text{oc})_6\text{Pd}(\text{cap})_6$  core with its two metal-uncapped *trans* octahedral  $\text{Pd}(\text{oc})_3$  faces additionally capped by iodide  $\mu_3\text{-I}$  atoms. The three tetracapping  $\mu_4\text{-I}$  atoms are each coordinated to two  $\text{Pd}(\text{oc})$  and two adjacent  $\text{Pd}(\text{cap})$  atoms. A comparative geometrical/qualitative bonding analysis of the hexacapped octahedral  $\text{Pd}(\text{oc})_6\text{Pd}(\text{cap})_6$  core in **1** with the structurally analogous cores in the recently reported  $\text{Pd}_{12}$  clusters,  $\text{Pd}_{12}(\mu_2\text{-CO})_6(\mu_3\text{-CO})_6(\text{PR}_3)_6$  ( $\text{R} = n\text{-Bu}$  (**4**), Ph (**5**)), revealed significantly different architectural features but yet emphasized the importance of the  $\text{Pd}(\text{cap})$  atoms in stabilizing the  $\text{Pd}(\text{oc})$  octahedra in **1**, **4**, and **5**. In fact, strong bonding interactions of the  $\mu_3\text{-I}$  and  $\mu_4\text{-I}$  atoms to the  $\text{Pd}_{12}$  polyhedron in **1** are evidenced by its black-violet crystals being air-stable for at least one month and by **1** dissolved in THF, acetone, or acetonitrile not undergoing decomposition to  $\text{AgI}$  upon addition of  $\text{Ag}(\text{OAc})$ . An exploration via the structure-to-synthesis approach of possible preparative pathways involving 14 different chemical reactions was carried out in order to isolate **1** in much higher yields. This systematic investigation demonstrated the importance of conproportionation reactions (i.e.,  $\text{Pd}(0) + \text{Pd}(\text{II}) \rightarrow \text{Pd}(\text{I}/2)$  in **1**) utilizing the co-products *trans*- $\text{Pd}_2(\mu_2\text{-I})_2\text{I}_2\text{L}_2$  (**7**) and *trans*- $\text{PdI}_2\text{L}_2$  (**8**), in different chemical reactions as palladium(II) precursors; high yields of **1** (ca. 50% based upon **6**) were obtained from conproportionation reactions in THF of palladium(0)  $\text{Pd}_{10}(\text{CO})_{12}\text{L}_6$  (**6**) with **7** in the presence of  $\text{Pd}(\text{OAc})_2$  and  $(\text{NBU}_4^+)(\text{PF}_6^-)$ . The square-planar palladium(II) geometries of the iodide-bridged dimeric **7** and monomeric **8** are compared with each other and with those of the previous crystallographically determined **8** (at room temperature) and several crystallographically known analogues (with different phosphine ligands); corresponding molecular parameters

\* Corresponding author.

E-mail address: [dahl@chem.wisc.edu](mailto:dahl@chem.wisc.edu) (L.F. Dahl).

were found to be in remarkably close agreement with distinct bond-length variations in bridging Pd–I(b) and terminal Pd–P bonds being readily attributed to the well-documented *trans* influence.

© 2004 Elsevier B.V. All rights reserved.

## 1. Introduction

Palladium halides (X = Cl, Br, I) and their derivatives constitute a widespread class of compounds, a number of which were originally utilized for palladium-catalyzed reactions. Although many of these palladium halide compounds possess two or more palladium atoms, the largest ones that are ligated primarily by terminal and/or doubly bridging  $\mu_2$ -X halide atoms contain less than eight metal atoms. Among *homopalladium* compounds, triply bridging  $\mu_3$ -X halide coordination has been observed for only a few 48-electron Pd<sub>3</sub> triangular clusters that are supported by *bidentate* ligands, such as Ph<sub>2</sub>PCH<sub>2</sub>PPh<sub>2</sub> (dppm) or Ph<sub>2</sub>AsCH<sub>2</sub>AsPh<sub>2</sub> (dpam); examples are [Pd<sub>3</sub>( $\mu_3$ -X)( $\mu_3$ -CO)( $\mu_2$ -dppm)<sub>3</sub>]<sup>+</sup> (X = Cl [1a,1b], I [1c]), [Pd<sub>3</sub>( $\mu_3$ -I)( $\mu_3$ -PF<sub>3</sub>)( $\mu_2$ -dppm)<sub>3</sub>]<sup>+</sup> [1d] and [Pd<sub>3</sub>( $\mu_3$ -I)( $\mu_3$ -CO)( $\mu_2$ -dpam)<sub>3</sub>]<sup>+</sup> [1e]. To our knowledge, there is only one recently reported  $\mu_3$ -X halide homopalladium cluster, Pd<sub>3</sub>( $\mu_3$ -Cl)<sub>2</sub>Cl<sub>3</sub>(PPh<sub>3</sub>)<sub>3</sub> [1f] that has *monodentate* phosphorus ligands. This 49-electron triangular *non-carbonyl* Pd<sub>3</sub> cluster is characterized by 0.2–0.3 Å longer Pd···Pd distances (range 3.064(1)–3.154(1) Å) [1f] indicative of weaker Pd–Pd bonding interactions. In striking contrast to the above 48-electron Pd<sub>3</sub> clusters with *bidentate* phosphorus ligands, Pd<sub>3</sub>( $\mu_3$ -Cl)<sub>2</sub>Cl<sub>3</sub>(PPh<sub>3</sub>)<sub>3</sub> contains much shorter (normal) Pd–( $\mu_3$ -Cl) distances for the two independent ( $\mu_3$ -Cl) ligands with means of 2.47 and 2.29(1) Å (i.e., this 0.18 Å difference was readily attributed to a strong *trans* effect) [1f] than those of 2.90 Å for [Pd<sub>3</sub>( $\mu_3$ -Cl)( $\mu_3$ -CO)( $\mu_2$ -dppm)<sub>3</sub>]<sup>+</sup> ([CF<sub>3</sub>CO<sub>2</sub>]<sup>−</sup> salt) [1a] and 2.86 Å for [Pd<sub>3</sub>( $\mu_3$ -Cl)( $\mu_3$ -CO)( $\mu_2$ -dppm)<sub>3</sub>]<sup>+</sup> ([BF<sub>4</sub>]<sup>−</sup> salt) [1b]. The abnormally long triply bridging Pd–( $\mu_3$ -Cl) distances in each of these latter two monocations were ascribed to very weak bonding and raised the question as to whether the linkage of the ( $\mu_3$ -Cl) ligand is entirely ionic or whether partial covalency is involved. In this connection, two comprehensive reviews by Puddephatt et al. [2] and Harvey and collaborators [3] provide an excellent detailed overview of the structures and bonding of these clusters together with their unusual catalytic, optical, and electrochemical properties and chemical reactivities. Both groups consider these and related clusters as halide *adducts* of the coordinatively unsaturated 42-electron [Pd<sub>3</sub>( $\mu_3$ -CO)( $\mu_2$ -dppm)<sub>3</sub>]<sup>2+</sup> *host*; they attribute the abnormally long distances between the palladium atoms and halide anions to steric effects caused by the phenyl rings of the *bidentate* dppm ligands that prevent close approaches of the halide *adducts* to normal distances.

For *heteronuclear* palladium clusters, which are not under consideration herein,  $\mu_3$ -X halide coordination was found in CoPd<sub>3</sub>( $\mu_3$ -X)( $\mu_2$ -CO)<sub>3</sub>( $\mu_3$ -CO)(CO)(PBu<sub>3</sub>)<sub>3</sub> (where X = Cl, Br, I) [4].

Among *carbonyl*-containing halide derivatives of *homonuclear* palladium compounds with *monodentate* phosphine ligands, only two kinds of clusters are known: namely, tetranuclear Pd<sub>4</sub>( $\mu_2$ -I)<sub>2</sub>( $\mu_2$ -CO)<sub>x</sub>(PPh<sub>3</sub>)<sub>4</sub> (where x = 2, 3) [5a] and hexanuclear Pd<sub>6</sub>( $\mu_2$ -X)<sub>4</sub>( $\mu_2$ -CO)<sub>4</sub>(PR<sub>3</sub>)<sub>4</sub> (where R = Ph, X = Cl [5b,5c] Br, [5b,5c] I [5a]; R = Bu<sup>t</sup>, X = Br, I [2]). Of the hexanuclear Pd<sub>6</sub> clusters, crystal structures were determined by X-ray diffraction studies for Pd<sub>6</sub>( $\mu_2$ -Cl)<sub>4</sub>( $\mu_2$ -CO)<sub>4</sub>(PPh<sub>3</sub>)<sub>4</sub> [5c] and Pd<sub>6</sub>( $\mu_2$ -Br)<sub>4</sub>( $\mu_2$ -CO)<sub>4</sub>(PBu<sup>t</sup>)<sub>4</sub> [4]. Each consists of two 44-electron triangular Pd<sub>3</sub>( $\mu_2$ -X)( $\mu_2$ -CO)<sub>2</sub>(PR<sub>3</sub>)<sub>2</sub> moieties that are only joined together by two additional doubly bridging ( $\mu_2$ -X) atoms (i.e., no Pd–Pd bond). The two Pd<sub>3</sub>( $\mu_2$ -Cl)( $\mu_2$ -CO)<sub>2</sub>(PPh<sub>3</sub>)<sub>2</sub> triangles in the former centrosymmetric Pd<sub>6</sub> cluster are oriented in an *anti* conformation with an overall pseudo-C<sub>2h</sub> molecular geometry, whereas the two Pd<sub>3</sub>( $\mu_2$ -Br)( $\mu_2$ -CO)<sub>2</sub>(PBu<sup>t</sup>)<sub>2</sub> triangles in the latter Pd<sub>6</sub> cluster are in a *syn* conformation with an overall pseudo-C<sub>2v</sub> molecular geometry.

Of particular interest is the reversible chemical transformation, characterized from TLC, IR, and UV-vis measurements, of the tetranuclear 58-electron Pd<sub>4</sub>( $\mu_2$ -I)<sub>2</sub>( $\mu_2$ -CO)<sub>2</sub>(PPh<sub>3</sub>)<sub>4</sub> into the 60-electron Pd<sub>4</sub>( $\mu_2$ -I)<sub>2</sub>( $\mu_2$ -CO)<sub>3</sub>(PPh<sub>3</sub>)<sub>4</sub> that occurs in solution by the rapid addition of one bridging carbonyl ligand under a CO atmosphere; however, this bridging CO ligand can then be removed under an Ar atmosphere to generate the original Pd<sub>4</sub>( $\mu_2$ -I)<sub>2</sub>( $\mu_2$ -CO)<sub>2</sub>(PPh<sub>3</sub>)<sub>4</sub> cluster [5a]. Although their solid-state molecular structures have not as yet been established from X-ray crystallographic studies, analogous crystallographically characterized palladium carbonyl/phosphine clusters are known; these include the 58-electron butterfly-shaped Pd<sub>4</sub>( $\mu_2$ -CO)<sub>5</sub>(PPh<sub>3</sub>)<sub>4</sub> [6a,6b] and Pd<sub>4</sub>( $\mu_2$ -CO)<sub>5</sub>(PPh<sub>2</sub>Me)<sub>4</sub> [6c], and the 60-electron tetrahedral-shaped Pd<sub>4</sub>( $\mu_2$ -CO)<sub>6</sub>(PBu<sup>n</sup>)<sub>4</sub> [6d]. Furthermore, conversion of Pd<sub>4</sub>( $\mu_2$ -CO)<sub>5</sub>(PBu<sup>n</sup>)<sub>4</sub> into Pd<sub>4</sub>( $\mu_2$ -CO)<sub>6</sub>(PBu<sup>n</sup>)<sub>4</sub> under CO atmosphere has been observed [6d,6e].

Systematic exploration (by E.G.M.) of various synthetic pathways for obtaining triphenylphosphine Pd<sub>4</sub>( $\mu_2$ -I)<sub>2</sub>( $\mu_2$ -CO)<sub>x</sub>(PPh<sub>3</sub>)<sub>4</sub> (x = 2, 3) and Pd<sub>6</sub>( $\mu_2$ -I)<sub>4</sub>( $\mu_2$ -CO)<sub>4</sub>(PPh<sub>3</sub>)<sub>4</sub> compounds gave rise to several different reaction routes including: (a) direct iodination of Pd<sub>n</sub>(CO)<sub>x</sub>(PPh<sub>3</sub>)<sub>y</sub> clusters; (b) conproportionation reactions of zerovalent Pd<sub>n</sub>(CO)<sub>x</sub>(PPh<sub>3</sub>)<sub>y</sub> clusters with square-planar palladium(II) PdI<sub>2</sub>(PPh<sub>3</sub>)<sub>2</sub>; (c) oxidative

addition of iodophosphorane,  $R_3PI_2$ <sup>1, 2</sup> [7,8], to  $Pd_n(CO)_x(PR_3)_y$  ( $R = Ph$ ); and (d) reduction of  $Pd(OAc)_2$  by CO in the presence of  $PPh_3$  and iodide anions [5a].

Our research interests at UW-Madison have unexpectedly become intertwined with the above findings. During systematic studies in chemistry of two thallium–palladium carbonyl/phosphine clusters,  $(\mu_6-Tl)[Pd_3(\mu_2-CO)_3L_3]_2^+$  (**2**) [9] and  $[Tl_2Pd_{12}(\mu_2-CO)_6(\mu_3-CO)_3L_9]^{2+}$  (**3**) [10] ( $L = PET_3$ ;  $[PF_6]^-$  salts), we found that reaction of the labile sandwich **2** with  $I_2$  gives (in small yields) the unusual  $[Pd_{12}(\mu_3-I)_2(\mu_4-I)_3(\mu_2-CO)_6(PET_3)_6]^+$  monocation (**1**), (isolated as the  $[PF_6]^-$  salt). As soon as its composition was unambiguously provided from an X-ray crystallographic determination, we then successfully modified and applied via a structure-to-synthesis approach several different preparative pathways (mentioned above [5a] for previously isolating the triphenylphosphine “ $Pd_4(\mu_2-I)_2$ ” and “ $Pd_6(\mu_2-I)_4$ ” clusters), which in most cases produced **1** in reasonable yields.

This 12-atom metal-core monocation (**1**) represents an initial example of a high-nuclearity halide-containing carbonyl/phosphine cluster of palladium (arbitrarily designated by us to have a minimum of 10 metal atoms with direct metal-metal bonding connectivities). Our investigation reported herein includes not only several different synthetic routes to **1** but also its stereochemical and spectroscopic characterization.

## 2. Results and discussion

### 2.1. Solid-state structure of $[Pd_{12}(\mu_3-I)_2(\mu_4-I)_3(\mu_2-CO)_6(PET_3)_6]^+$ (**1**)

#### 2.1.1. General comments

The consecutive build-up scheme of **1** with its crystallographically imposed trigonal  $D_3$  (32) molecular geometry is shown in Fig. 1(a)–(e). A comparison of its connectivities is given in Table 1, for which a given connectivity is identified in Fig. 1 from the atom-labeling of a specified individual atom-pair; the number of symmetry-equivalent distances under  $D_3$  symmetry for a given connectivity is also presented in Table 1.

<sup>1</sup> Crystallographic X-ray studies of iodophosphorane  $R_3PI_2$  species have shown (to date) that phosphorus possesses a tetrahedral-like  $R_3P-I-I$  geometry in the solid state; these include  $R_3 = (t-Bu)_3$  [7a],  $Ph_3$  [7b],  $PhMe_2$  [7c], and  $[2,4,6-(CH_3O)_3C_6H_2]_3$  [7d].

<sup>2</sup> Because we used an excess amount of  $I_2$ , it also should be noted that iodophosphoranes  $R_3PI_2$  are able to react with additional free iodine to form iodophosphonium triiodide  $R_3PI^+I_3^-$  ions and their dimeric derivatives  $[(R_3PI)_2I_3]^+I_3^-$  with different solid-state structures that are influenced by the nature of the R substituents and solvents. Crystallographically characterized examples are  $[(PPh_3)_2I_3]I_3$  [8a],  $(PPh_3)I_3$  [8a],  $[(PPR'_3)_2I_3]I_3$  [8b], and  $[(Pr'_2N)_3PI]I_3$  [8b].

Fig. 1(c) and (d) shows that the principal  $C_3$ -axis passes through the two tricapping  $\mu_3-I$  atoms, while each of the three horizontal  $C_2$ -axes passes through one of the three tetracapping  $\mu_4-I$  atoms and the midpoints of two *trans*-oriented  $Pd(oc)-Pd(oc)$  bond-edges of the octahedral  $Pd(oc)_6$  kernel. The resulting crystallographically asymmetric unit is one-sixth of the monocation (**1**).

#### 2.1.2. $Pd_{12}$ core

Its 12-atom metal core can be considered as a distorted hexacapped  $Pd(oc)_6Pd(cap)_6$  octahedron composed of an octahedral  $Pd(n)$  kernel ( $n = 1, 1A, 1B, 1C, 1D, 1E$ ) that is triangularly capped by six  $Pd(n)$  atoms ( $n = 2, 2A, 2B, 2C, 2D, 2E$ ); each of these six capping Pd atoms is connected to a  $PET_3$  ligand (Fig. 1(a) and (b)). The remaining two metal-uncapped triangular *trans*- $Pd(oc)_3$  faces of the  $Pd(n)$  octahedron (namely, those with  $n = 1, 1B, 1D$  and  $n = 1A, 1C, 1E$ ) may be designated as two symmetry-equivalent *intralayer* (basal) equilateral triangles with one independent bonding  $Pd(oc)-Pd(oc)$  distance of 2.840(1) Å within each basal  $Pd(oc)_3$  triangle and two independent bonding  $Pd(oc)-Pd(oc)$  distances of 2.821(1) and 2.949(1) Å between the basal  $Pd(oc)_3$  triangles. The  $Pd(oc)_6Pd(cap)_6$  core is formally constructed by the capping of each of the six *interlayer* triangular  $Pd(oc)_3$  faces connecting the two basal triangles with  $Pd(cap)$  atoms; the resulting 18 bonding  $Pd(oc)-Pd(cap)$  distances consist of three independent ones of 2.721(1), 2.768(1), and 2.948(1) Å. This hexacapped octahedral  $Pd_{12}$  core of **1** can also be envisioned as two stacked intralayers of non-planar  $v_2 Pd_6$  triangles (where  $v_2$  designates 3 equally spaced atoms along each edge) composed of  $Pd(n)$  with  $n = 2, 1B, 2B, 1D, 2D, 1$  and  $n = 2A, 1C, 2C, 1E, 2E, 1A$ ; these two stacked  $Pd_6$  layers conform to a trigonal-antiprismatic geometry with a twist angle about the principal threefold axis deviating from a regular staggered conformation by 6.3° (Fig. 1(a)). Each of the three outer  $Pd(n)$ -capping atoms in the two layers (namely, those with  $n = 2, 2B, 2D$  and  $n = 2A, 2C, 2E$ ) is displaced from its corresponding basal octahedral plane (defined by the three inner Pd atoms with  $n = 1, 1B, 1D$  and  $n = 1A, 1C, 1E$ ) toward the opposite basal octahedral  $Pd(oc)_3$  triangle; the resulting angle between  $Pd(n)$ ,  $n = 1, 2, 1B$  and  $n = 1, 1B, 1D$  planes and the other five symmetry-equivalent corresponding pairs is 5.4°. These significant geometrical deviations are ascribed primarily to the combined steric/electronic effects of the three  $\mu_4-I$  atoms and six  $\mu_2-CO$  ligands (vide infra).

#### 2.1.3. $Pd_{12}(\mu_3-I)_2(\mu_4-I)_3$ fragment

The two oppositely directed triangular basal  $Pd(oc)_3$  faces (normal to the pseudo-threefold axis) are capped by two  $\mu_3-I$  ligands with the six symmetry-equivalent  $Pd(oc)-(\mu_3-I)$  distances being 2.757(1) Å.

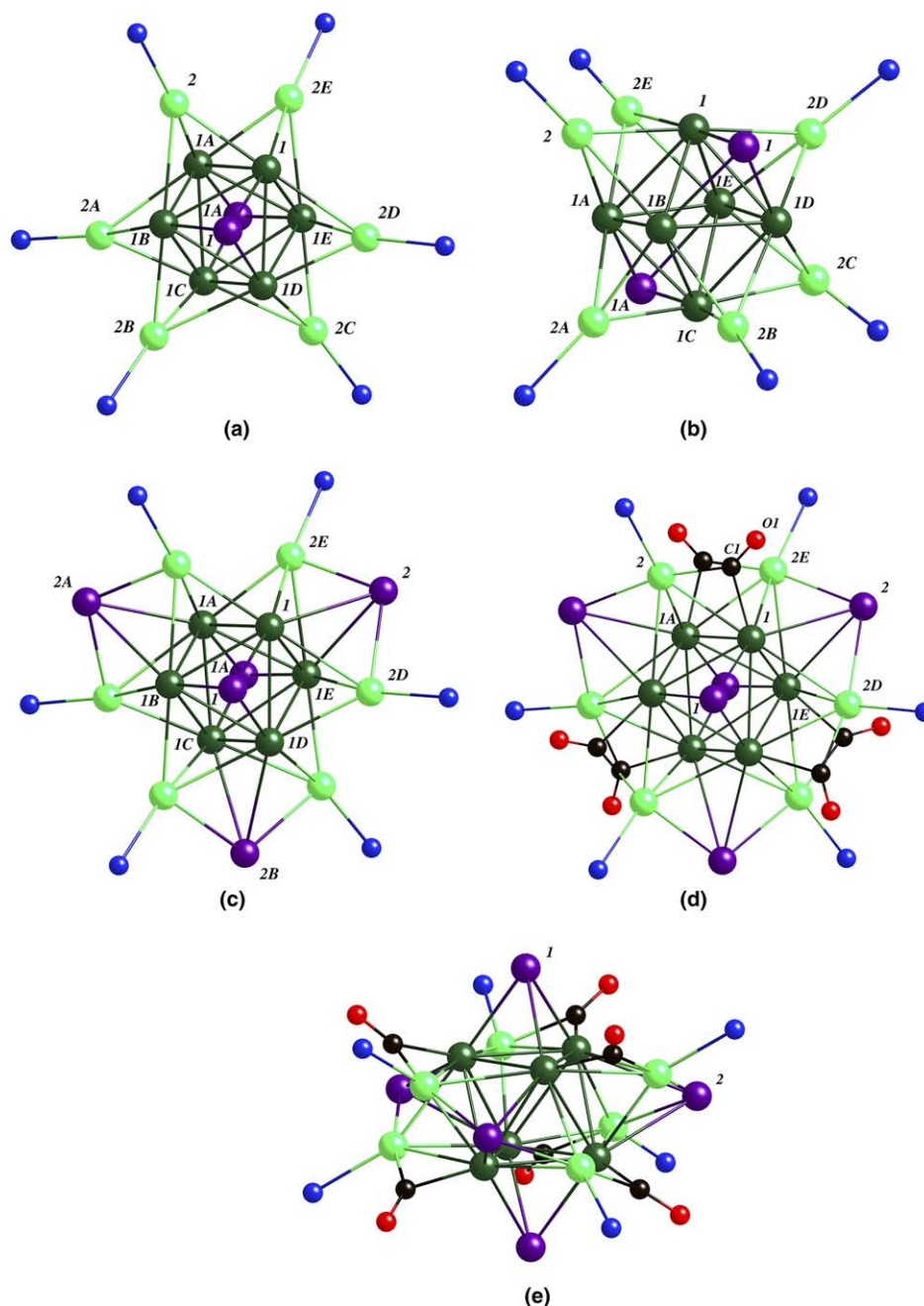


Fig. 1. The consecutive build-up scheme of  $[\text{Pd}_{12}(\mu_3\text{-I})_2(\mu_4\text{-I})_3(\mu_2\text{-CO})_6\text{L}_6]^+$  monocation (**1**) ( $\text{L} = \text{PEt}_3$ ;  $[\text{PF}_6]^-$  salt) of crystallographic  $D_3$  ( $32$ ) site symmetry: (a) top and (b) side views, respectively, of the octacapped octahedral  $\text{Pd}_6(\mu_3\text{-Pd})_6(\mu_3\text{-I})_2\text{P}_6$  fragment formally constructed from the central  $\text{Pd}(\text{oc})_6$  octahedron by the capping of six of its triangular faces with  $\text{Pd}(\text{cap})\text{P}$  groups and the remaining two *trans* triangular faces with  $\mu_3\text{-I}$  atoms; (c) top view displaying the additional tetracapping of the octacapped octahedral  $\text{Pd}(\text{oc})_6\text{Pd}(\text{cap})_6(\mu_3\text{-I})_2\text{P}$  fragment with three  $\mu_4\text{-I}$  atoms, each having a localized butterfly-shaped coordination consisting of two hinge  $\text{Pd}(\text{oc})$  atoms and two wingtip  $\text{Pd}(\text{cap})$  atoms; (d) and (e) top and side views, respectively, of the entire structure (without phosphorus-attached ethyl substituents) formed by the addition of the 12 symmetry-equivalent edge-bridging  $\mu_2\text{-CO}$  ligands that span  $\text{Pd}(\text{oc})\text{-Pd}(\text{cap})$  edges of the other three unoccupied butterfly-shaped  $\text{Pd}(\text{oc})_2\text{Pd}(\text{cap})_2$  fragments.  $\text{Pd}(\text{oc})$  atoms are dark green;  $\text{Pd}(\text{cap})$  atoms, light green;  $\mu_3\text{-I}$  and  $\mu_4\text{-I}$  atoms, purple; carbon atoms, black; and oxygen atoms, red.

Each of the threefold-related tetracapping  $\mu_4\text{-I}$  atoms is coordinated to a localized butterfly-shaped  $\text{Pd}(\text{oc})_2\text{Pd}(\text{cap})_2$  fragment composed of two twofold-related basal  $\text{Pd}(\text{oc})$  atoms and two twofold-related wingtip  $\text{Pd}(\text{cap})$  atoms; the determined independent  $\text{Pd}(\text{cap})\text{-}(\mu_4\text{-I})$  distances are 3.110(1) and 2.634(1) Å.

Addition of the three tetracapping  $\mu_4\text{-I}$  atoms (and six doubly bridging  $\mu_2\text{-CO}$  ligands and 18 phosphorus-attached ethyl substituents) gives rise to a large deformation of the  $\text{Pd}_6(\mu_3\text{-Pd})_6(\mu_3\text{-I})_2\text{P}_6$  fragment from pseudo-centrosymmetric  $D_{3d}$  ( $32/m$ ) symmetry to the observed crystallographic  $D_3$  symmetry (i.e., involving

Table 1  
Comparison of connectivities (Å) for  $[\text{Pd}_{12}(\mu_3\text{-I})_2(\mu_4\text{-I})_3(\mu_2\text{-CO})_6(\text{PET}_3)_6]^+$  (**1**) under crystallographic  $D_3$  site symmetry

Connectivity <sup>a</sup>	Individual atom-pair <sup>b</sup>	$N^c$	Distance
Pd(oc)–Pd(oc) (within basal triangles)	Pd(1)–Pd(1B)	6	2.840(1)
Pd(oc)–Pd(oc) (between basal triangles)	Pd(1)–Pd(1E)	3	2.821(1)
Pd(oc)–Pd(oc) (between basal triangles)	Pd(1)–Pd(1A)	3	2.949(1)
Pd(oc)–Pd(cap) (interlayer)	Pd(1A)–Pd(2)	6	2.721(1)
Pd(oc)–Pd(cap) (intralayer)	Pd(1)–Pd(2)	6	2.768(1)
Pd(oc)–Pd(cap) (intralayer)	Pd(1B)–Pd(2)	6	2.948(1)
Pd(cap)···Pd(cap)	Pd(2)···Pd(2A)	3	4.267(2)
Pd(cap)···Pd(cap)	Pd(2)···Pd(2E)	3	3.334(2)
Pd(oc)–( $\mu_3\text{-I}$ )	Pd(1)–I(1)	6	2.757(1)
Pd(oc)–( $\mu_4\text{-I}$ )	Pd(1)–I(2)	6	3.110(1)
Pd(cap)–( $\mu_4\text{-I}$ )	Pd(2E)–I(2)	6	2.634(1)
Pd(cap)–P	Pd(2)–P	6	2.290(3)
Pd(oc)–( $\mu_2\text{-CO}$ )	Pd(1)–C(1)	6	1.97(1)
Pd(cap)–( $\mu_2\text{-CO}$ )	Pd(2)–C(1)	6	1.96(1)
C–O	C(1)–O(1)	6	1.15(1)

<sup>a</sup> Pd(oc) and Pd(cap) designate the six symmetry-equivalent octahedral and capping palladium atoms, respectively. The two basal triangles denote the two opposite (*trans*-oriented) triangular Pd(oc)<sub>3</sub> faces of the octahedral Pd<sub>6</sub> kernel that are not capped by Pd(cap) atoms (i.e., they are instead capped by the two  $\mu_3\text{-I}$  atoms).

<sup>b</sup> Atom-labeling is given in Fig. 1.

<sup>c</sup>  $N$  denotes the number of symmetry-equivalent connectivities under  $D_3$  symmetry.

loss of both the inversion center  $i$  and the three vertical  $\sigma_d$  mirror planes that bisect the pairs of three horizontal  $C_2$ -axes). Steric/electronic consequences are evidenced by the two wingtip Pd(cap) atoms of the ( $\mu_4\text{-I}$ )-occupied butterfly-shaped fragment being separated by a much longer non-bonding Pd(cap)···Pd(cap) distance of 4.267(2) Å compared to that of 3.334(2) Å for the two wingtip Pd(cap) atoms of the other three symmetry-equivalent unoccupied butterfly-shaped fragments.

## 2.2. Geometrical bonding relationship of the hexacapped octahedral Pd<sub>12</sub> core in $[\text{Pd}_{12}(\mu_3\text{-I})_2(\mu_4\text{-I})_3(\mu_2\text{-CO})_6(\text{PET}_3)_6]^+$ (**1**) with the hexacapped octahedral Pd<sub>12</sub> core in two isostructural $[\text{Pd}_{12}(\text{CO})_{12}(\text{PR}_3)_6]$ clusters ( $R = n\text{-Bu}$ (**4**), $\text{Ph}$ (**5**))

A comparison of the Pd<sub>6</sub>( $\mu_3\text{-Pd}$ )<sub>6</sub> core geometry of **1** with those of the recently reported isostructural Pd<sub>12</sub> clusters, Pd<sub>12</sub>( $\mu_2\text{-CO}$ )<sub>6</sub>( $\mu_3\text{-CO}$ )<sub>6</sub>(PR<sub>3</sub>)<sub>6</sub> ( $R = n\text{-Bu}$  (**4**) [11], Ph (**5**) [12]) is informative. These latter two molecular clusters (represented in Fig. 2 by the triphenylphosphine **5**), which were isolated from entirely different synthetic routes, possess essentially identical geometries (other than the different phosphorus-attached substituents); corresponding means for their Pd<sub>6</sub>( $\mu_3\text{-Pd}$ )<sub>6</sub> cores vary by less than 0.02 Å except for the weakly bonding

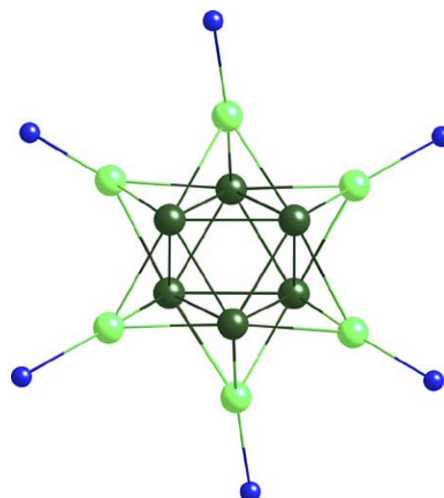


Fig. 2. Centrosymmetric architecture of the Pd(oc)<sub>6</sub>Pd(cap)<sub>6</sub>P<sub>6</sub> fragment in the two known isostructural Pd<sub>12</sub>( $\mu_2\text{-CO}$ )<sub>6</sub>( $\mu_3\text{-CO}$ )<sub>6</sub>(PR<sub>3</sub>)<sub>6</sub> clusters ( $R = n\text{-Bu}$  (**4**) [11], Ph (**5**) [12]). Each of their essentially identical molecular geometries (other than the different R substituents) of crystallographic  $C_i$  ( $\bar{1}$ ) site symmetry ideally conforms to centrosymmetric  $D_{3d}$  ( $32/m$ ) symmetry.

(or non-bonding) *interlayer* Pd(oc)–Pd(oc) means which differ by 0.06 Å (vide infra). Particularly noteworthy is that the molecular geometry for **4** and also for **5** has crystallographically  $C_i$  ( $\bar{1}$ ) site symmetry and that addition of the P atoms (without substituents) and CO ligands to its Pd<sub>12</sub> core preserves the centrosymmetric pseudo- $D_{3d}$  ( $32/m$ ) symmetry.

In contradistinction, the Pd<sub>6</sub>( $\mu_3\text{-Pd}$ )<sub>6</sub>( $\mu_3\text{-I}$ )<sub>2</sub>P<sub>6</sub> fragment in **1** is greatly deformed (as previously mentioned) from pseudo- $D_{3d}$  to crystallographic  $D_3$  symmetry because of the non-conformity of the three  $\mu_4\text{-I}$  and six  $\mu_2\text{-CO}$  ligands to  $D_{3d}$  symmetry. Visual evidence for the much greater geometric distortions of the Pd<sub>12</sub> core in **1** is shown from a comparison of Figs. 1 and 2. Apparent differences include the two symmetry-identical *intralayers* in **4** and **5** being centrosymmetrically oriented in a staggered close-packed array such that the two *interlayer* Pd(oc) triangles of the Pd(oc)<sub>6</sub> kernel form a regular trigonal antiprism with the six *interlayer* Pd(cap) atoms being equally separated; in sharp contrast, the six Pd(cap) atoms in **1** are irregularly separated (Fig. 1) due primarily to steric effects involving the three tetracapping  $\mu_4\text{-I}$  atoms (vide supra). The resulting major structural variation between **1** and **4** (**5**) is that the average framework of the inner Pd(oc)<sub>6</sub> kernels in **4** (**5**) is much more deformed from an octahedral toward a regular trigonal-antiprismatic geometry due to a considerably greater elongation of the six *interlayer* Pd(oc)–Pd(oc) distances (between basal triangles) with resulting means of 3.23 (3.17) Å for **4** (**5**) versus 2.82 and 2.95 Å for the corresponding non-equivalent means (under  $D_3$  symmetry) for **1**. The bonding 12 *intralayer* and six *interlayer* Pd(cap)–Pd(oc) means of 2.81 (2.82)

and 2.70 (2.72) Å, respectively, for **4** (**5**) versus 12 *intra-layer* ones of 2.77 and 2.95 Å and six *interlayer* ones of 2.72 Å for **1** are in accordance with Pd(cap) atoms stabilizing the Pd(oc)<sub>6</sub> kernels in both **1** and **4** (**5**) via Pd(cap)–Pd(oc) bonding interactions.

An examination of predicted electron counts for the octacapped octahedral Pd<sub>6</sub>(μ<sub>3</sub>-Pd)<sub>6</sub>(μ<sub>3</sub>-I)<sub>2</sub> fragment in **1** compared to the hexacapped octahedral Pd<sub>6</sub>(μ<sub>3</sub>-Pd)<sub>6</sub> core in **4** (**5**) provides a qualitative indication concerning their overall bonding differences. If the Pd<sub>12</sub> core in **4** (**5**) is considered as a hexacapped octahedron, the cluster valence electron count is 84 CVEs (i.e., 6 × 10 (Pd(oc)) + 6 × 0 (Pd(cap)PR<sub>3</sub>) + 12 × 2 (CO) = 84). The corresponding electron count for the octacapped octahedron in **1** is not unambiguous due to the donor contribution of each μ<sub>4</sub>-I atom (designated “n”) not being straightforward [i.e., 6 × 10 (Pd(oc)) + 6 × 0 (Pd(cap)-PEt<sub>3</sub>) + 2 × 5 (μ<sub>3</sub>-I) + 3 × n (μ<sub>4</sub>-I) + 2 × 6 (CO) – 1 (charge) = 81 + 3n(μ<sub>4</sub>-I) CVEs]. If each μ<sub>4</sub>-I ligand is assumed to donate five of its seven valence electrons (i.e., n = 5), the resulting electron count of 96 CVEs is abnormally high and unrealistic for Pd-capped Pd<sub>6</sub> octahedral clusters. In any event, this qualitative electron-count scheme supports our view that the iodide-coordinated **1** is an electron-rich cluster.

### 2.3. Synthesis of [Pd<sub>12</sub>(μ<sub>3</sub>-I)<sub>2</sub>(μ<sub>4</sub>-I)<sub>3</sub>(μ<sub>2</sub>-CO)<sub>6</sub>L<sub>6</sub>]<sup>+</sup> (**1**) (L = PEt<sub>3</sub>; [PF<sub>6</sub>]<sup>−</sup> salt) from different preparative pathways

#### 2.3.1. General comments

Based upon the crystallographically determined structure and composition of **1**, which was originally obtained in low yield from the reaction of the labile (μ<sub>6</sub>-Tl)[Pd<sub>3</sub>(μ<sub>2</sub>-CO)<sub>3</sub>L<sub>3</sub>]<sub>2</sub><sup>+</sup> sandwich (**2**) (L = PEt<sub>3</sub>; [PF<sub>6</sub>]<sup>−</sup> salt), a systematic exploration of possible synthetic routes via the structure-to-synthesis approach was carried out in order to isolate **1** in much higher yields. Table 2 provides a summary of the reactants and boundary conditions of 14 different reactions carried out at room temperature in THF along with the estimated yields of the crystalline products. In most cases **1** was obtained in reasonable yields.

#### 2.3.2. Direct iodination of heterometallic triethylphosphine palladium/thallium Pd<sub>6</sub>Tl (**2**) and Pd<sub>12</sub>Tl<sub>2</sub> (**3**) clusters and the homometallic triethylphosphine Pd<sub>10</sub> cluster (**6**)

Entries 1–3 in Table 2 show that **1** as the [PF<sub>6</sub>]<sup>−</sup> salt was isolated from reactions of I<sub>2</sub> with (μ<sub>6</sub>-Tl)[Pd<sub>3</sub>(μ<sub>2</sub>-CO)<sub>3</sub>L<sub>3</sub>]<sub>2</sub><sup>+</sup> (**2**) [9] and [Tl<sub>2</sub>Pd<sub>12</sub>(CO)<sub>9</sub>L<sub>9</sub>]<sup>2+</sup> (**3**) [10], and with Pd<sub>10</sub>(CO)<sub>12</sub>L<sub>6</sub> (**6**) [6e,13] in the presence of

Table 2

Summary of reactants, reaction conditions, and estimated yields of crystalline products for 14 different reactions performed at room temperature in THF in an exploration of possible synthetic routes to generate [Pd<sub>12</sub>I<sub>5</sub>(CO)<sub>6</sub>L<sub>6</sub>]<sup>+</sup> monocation (**1**) as [PF<sub>6</sub>]<sup>−</sup> salt (L = PEt<sub>3</sub>)

Number of entry	Reactants and their stoichiometry	Quantity of reactant cluster (mmol)	Atmosphere	Yields of crystalline products (%)		
				[Pd <sub>12</sub> I <sub>5</sub> (CO) <sub>6</sub> L <sub>6</sub> ] <sup>+</sup> [PF <sub>6</sub> ] <sup>−</sup> ( <b>1</b> )	Pd <sub>2</sub> I <sub>4</sub> L <sub>2</sub> ( <b>7</b> )	PdI <sub>2</sub> L <sub>2</sub> ( <b>8</b> )
1	(μ <sub>6</sub> -Tl)[Pd <sub>3</sub> (CO) <sub>3</sub> L <sub>3</sub> ] <sub>2</sub> [PF <sub>6</sub> ] <sup>−</sup> + 4.5I <sub>2</sub>	0.05	N <sub>2</sub>	5	32	17
2 <sup>a</sup>	[Tl <sub>2</sub> Pd <sub>12</sub> (CO) <sub>9</sub> L <sub>9</sub> ][PF <sub>6</sub> ] <sup>2+</sup> + 6I <sub>2</sub>	0.06	N <sub>2</sub>	8	3	17
3 <sup>a</sup>	Pd <sub>10</sub> (CO) <sub>12</sub> L <sub>6</sub> + Pd <sub>2</sub> dba <sub>3</sub> + 3.5I <sub>2</sub> + 2(NBu <sub>4</sub> <sup>n</sup> )PF <sub>6</sub>	0.05	N <sub>2</sub>	3 <sup>b</sup>	6 <sup>b</sup>	6 <sup>b</sup>
4	Pd <sub>10</sub> (CO) <sub>12</sub> L <sub>6</sub> + 3Pd <sub>2</sub> I <sub>4</sub> L <sub>2</sub> + 4Pd <sub>2</sub> dba <sub>3</sub> + 4(NH <sub>4</sub> )(PF <sub>6</sub> )	0.03	N <sub>2</sub>	35 <sup>b</sup> , 15 <sup>c</sup>	0	<sup>d</sup>
5	Pd <sub>10</sub> (CO) <sub>12</sub> L <sub>6</sub> + 3Pd <sub>2</sub> I <sub>4</sub> L <sub>2</sub> + 4Pd <sub>2</sub> dba <sub>3</sub> + 4(NH <sub>4</sub> )(PF <sub>6</sub> )	0.02	CO, 0.5 min; then N <sub>2</sub>	67 <sup>b</sup> , 28 <sup>c</sup>	0	<sup>d</sup>
6 <sup>c</sup>	Pd <sub>10</sub> (CO) <sub>12</sub> L <sub>6</sub> + 3Pd <sub>2</sub> I <sub>4</sub> L <sub>2</sub> + 4Pd <sub>2</sub> dba <sub>3</sub> + 4(NH <sub>4</sub> )(PF <sub>6</sub> )	0.02	CO	45 <sup>b</sup> , 19 <sup>c</sup>	0	18 <sup>b</sup>
7 <sup>f</sup>	6PdI <sub>2</sub> L <sub>2</sub> + 9Pd <sub>2</sub> dba <sub>3</sub> + 4(NH <sub>4</sub> )(PF <sub>6</sub> )		N <sub>2</sub> , 3 min; then CO	3 <sup>c</sup>	0	34 <sup>g</sup>
8	Pd <sub>10</sub> (CO) <sub>12</sub> L <sub>6</sub> + 2Pd <sub>2</sub> I <sub>4</sub> L <sub>2</sub> + Pd(OAc) <sub>2</sub> + 2(NH <sub>4</sub> )(PF <sub>6</sub> )	0.05	N <sub>2</sub>	54 <sup>b</sup>	0	21 <sup>b</sup> , 53 <sup>h</sup>
9	Pd <sub>10</sub> (CO) <sub>12</sub> L <sub>6</sub> + 4PdI <sub>2</sub> L <sub>2</sub> + 2(NH <sub>4</sub> )(PF <sub>6</sub> )	0.05	N <sub>2</sub>	17 <sup>b</sup>	0	57 <sup>g</sup>
10	Pd <sub>10</sub> (CO) <sub>12</sub> L <sub>6</sub> + 3PdI <sub>2</sub> L <sub>2</sub> + 3Pd(OAc) <sub>2</sub> + 2(NH <sub>4</sub> )(PF <sub>6</sub> )	0.05	N <sub>2</sub>	47 <sup>b</sup>	0	24 <sup>g</sup>
11	Pd <sub>10</sub> (CO) <sub>12</sub> L <sub>6</sub> + I <sub>2</sub> + 2Pd <sub>2</sub> I <sub>4</sub> L <sub>2</sub> + 2(NH <sub>4</sub> )(PF <sub>6</sub> )	0.05	N <sub>2</sub>	15 <sup>b</sup> , 12 <sup>c</sup>	0	27 <sup>b</sup> , 68 <sup>h</sup>
12	Pd <sub>10</sub> (CO) <sub>12</sub> L <sub>6</sub> + I <sub>2</sub> + 2Pd <sub>2</sub> I <sub>4</sub> L <sub>2</sub> + 2(NH <sub>4</sub> )(PF <sub>6</sub> )	0.05	CO	4 <sup>b</sup> , 3 <sup>c</sup>	0	43 <sup>b</sup> , 110 <sup>h</sup>
13	2Pd <sub>4</sub> (CO) <sub>5</sub> L <sub>4</sub> + 4.6Pd <sub>2</sub> I <sub>4</sub> L <sub>2</sub> + (NH <sub>4</sub> )(PF <sub>6</sub> )	0.12	N <sub>2</sub>	13 <sup>i</sup>	33 <sup>h</sup>	69 <sup>i</sup> , 59 <sup>h</sup>
14	Pd(OAc) <sub>2</sub> + CO + 0.5L + 0.4KI + 4(NH <sub>4</sub> )(PF <sub>6</sub> )	1.00 <sup>j</sup>	CO	1.6	0	12

<sup>a</sup> Small amounts (<2 mg) of colorless crystals were observed but not further investigated.

<sup>b</sup> Based on Pd<sub>10</sub>(CO)<sub>12</sub>L<sub>6</sub>.

<sup>c</sup> Based on all palladium reactants.

<sup>d</sup> Observed but not defined quantitatively.

<sup>e</sup> Solution of Pd<sub>2</sub>dba<sub>3</sub> in CHCl<sub>3</sub> was added through stainless steel canula (without direct contact with CO gas) into THF solution of other reactants dissolved under CO.

<sup>f</sup> Solvent CHCl<sub>3</sub> used instead of THF.

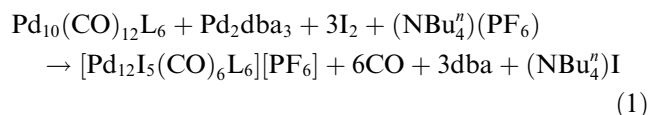
<sup>g</sup> Based on initial amount of PdI<sub>2</sub>L<sub>2</sub>.

<sup>h</sup> Based on Pd<sub>2</sub>I<sub>4</sub>L<sub>2</sub>.

<sup>i</sup> Based on Pd<sub>4</sub>(CO)<sub>5</sub>L<sub>4</sub>.

<sup>j</sup> mmol of Pd(OAc)<sub>2</sub>.

$\text{Pd}_2\text{dba}_3$  and  $(\text{NBu}_4^n)(\text{PF}_6)$  ( $L = \text{PEt}_3$ ; dba = dibenzylideneacetone). In the last reaction (entry 3),  $\text{Pd}_2\text{dba}_3$  was used to balance the idealized stoichiometry of the following reaction:



All three reactions are complicated by the formation of Pd black.

Hypothetically  $\text{I}_2$  could play the same role as  $\text{O}_2$  for enlargement of the  $\text{Pd}_n$ -core sizes of  $\text{Pd}_n(\text{CO})_x(\text{PR}_3)_y$  clusters by oxidative deligation of  $\text{PR}_3$  ligands with formation of phosphorane  $\text{R}_3\text{PI}_2$  species (analogous to the formation of  $\text{R}_3\text{PO}$  species upon reaction with  $\text{O}_2$  [14]); this potential synthetic pathway would involve the intermediate generation of coordinatively unsaturated palladium intermediates which would then oligomerize to larger palladium clusters. But in contrast to  $\text{O}_2$ , reactions with iodine normally result in the oxidation of Pd(0) into Pd(II) species that are stabilized by formation of strong Pd–I bonds. Thus, reactions with iodine (entries 1–3) gave rise to only small yields of **1** due largely to the formation of the stable square-planar palladium(II) *trans*- $\text{Pd}_2\text{I}_4(\text{PEt}_3)_2$  (**7**) and *trans*- $\text{PdI}_2(\text{PEt}_3)_2$  (**8**); both **7** and **8** were identified from  $^{31}\text{P}\{^1\text{H}\}$  NMR and complete X-ray structural analyses. It should be noted that formation of **7** and **8** could have occurred not only from direct oxidation by  $\text{I}_2$  of the zerovalent palladium atoms in the reactants **2**, **3** and **6** but also from secondary in situ oxidation reactions with the expectedly formed iodophosphorane  $\text{Et}_3\text{PI}_2$  or  $\text{Et}_3\text{PI}_4$  species (see footnotes 1 and 2) [7,8]. In fact, a fast reaction between  $\text{R}_3\text{PI}_2$  ( $\text{R} = \text{Ph}$  and  $\text{Pd}_{10}(\text{CO})_{12}(\text{PPh}_3)_6$ ) under CO atmosphere was previously reported to give  $\text{Pd}_4(\mu_2\text{-I})_2(\mu_2\text{-CO})_3(\text{PPh}_3)_4$  [5a]. Furthermore, McAuliffe and co-workers [15] showed that reactions of iodophosphoranes with unactivated metal powders produced a variety of new and existing transition metal phosphine complexes.

Subsequent possible reactions between reactants **2**, **3** and **6** with the generated **7** and **8** must also be considered. Although a considerable number of reactions between triphenylphosphine  $\text{Pd}_n(\text{CO})_x(\text{PR}_3)_y$  clusters and palladium(II) halide compounds have previously been performed [5], analogous reactions are less likely to occur in the present cases because of the higher reactivities of **2**, **3** and **6** (especially that of **2** [9]) with  $\text{I}_2$  and their significant consumption at the initial stage of each of these reactions.

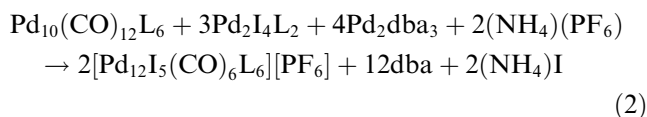
In general, molar ratios of  $\text{Pd}_n(\text{CO})_x(\text{PR}_3)_y/\text{I}_2$  should greatly affect the composition and yields of the products. For instance, reactions of  $\text{I}_2$  with triphenylphosphine  $\text{Pd}_4(\text{CO})_5(\text{PPh}_3)_4$  under Ar or CO atmosphere with a molar  $\text{Pd}_4/\text{I}_2$  ratio of 1:1 afforded the previously mentioned triphenylphosphine  $\text{Pd}_4\text{I}_2(\text{CO})_x(\text{PPh}_3)_4$  ( $x = 2$  or

3) clusters with estimated yields of 90% [5a]. Nevertheless, our attempts to decrease molar  $\text{Pd}_n/\text{I}_2$  ratios in reactions with **2**, **3**, or **6** did not result in higher yields of **1**.

It is apparent that the counterion  $[\text{PF}_6]^-$  plays a crucial role in the stabilization of the monocation (**1**). Thus, previous iodination reactions of the corresponding tributylphosphine  $\text{Pd}_{10}(\text{CO})_{12}(\text{PBu}_3^n)_6$  over a broad range of molar  $\text{Pd}_{10}/\text{I}_2$  ratios of 1/1–1/10 without counter ions gave no evidence for the formation of the analogous monocation (**1**) [5a].

### 2.3.3. Conproportionation reactions of zerovalent $\text{Pd}_{10}(\text{CO})_{12}(\text{PEt}_3)_6$ (**6**), $\text{Pd}_4(\text{CO})_5(\text{PEt}_3)_4$ , and $\text{Pd}_2\text{dba}_3$ with square-planar palladium(II) $\text{Pd}_2\text{I}_4\text{L}_2$ (**7**) and $\text{PdI}_2\text{L}_2$ (**8**) ( $L = \text{PEt}_3$ )

In further attempts to increase the yield of **1**, we developed another synthetic approach (Table 2, entries 4–6), based on the idealized stoichiometry of the following reaction:



In sharp contrast to the preparation of triethylphosphine **1** via direct oxidation with  $\text{I}_2$  (entries 1–3), reaction (2) utilizes as a *starting reagent* the undesirable *final product* of the previous reactions,  $\text{Pd}_2\text{I}_4(\text{PEt}_3)_2$  (**7**). Another major difference between reactions involving the direct oxidation with  $\text{I}_2$  is that the role of oxidant is carried out by palladium(II) (from  $\text{Pd}_2\text{I}_4\text{L}_2$ ) instead of  $\text{I}_2$  (Table 2, entries 4–6). Thus, reaction (2) is a conproportionation process involving changes in formal oxidation states of palladium from 0 and +2 in the precursors **6** and **7**, respectively, to that of +0.5 in **1**.

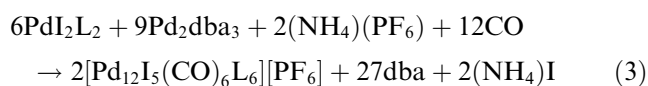
In spite of the fact that reaction (2) is again complicated by formation of Pd black, this different chemical route afforded much greater yields of **1** than that involving direct iodination of clusters **2**, **3**, **6** (compare entries 4–6 versus 1–3 in Table 2).

The other crystalline product of reaction (2) is the unexpected mononuclear 16-electron square-planar palladium(II) complex, *trans*- $\text{PdI}_2(\text{PEt}_3)_2$  (**8**). The observation of **8** was unanticipated because of the large (four times) deficiency of  $\text{PEt}_3$  necessary for its formation from reaction (2), in which the total molar Pd/ $\text{PEt}_3$  ratio of the reactants was 2/1.

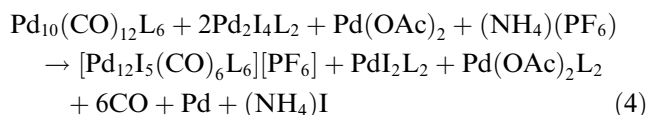
The sole source of CO for formation of **1** by reaction (2) (entry 4) is  $\text{Pd}_{10}(\text{CO})_{12}(\text{PEt}_3)_6$  (**6**). In reality the available amount of CO from **6** is not sufficient for the best yield of **1**, because carbonyl/phosphine clusters of palladium readily lose CO under an inert atmosphere [14b], especially in the presence of other reagents [14c]. In fact, the yield of **1** was found to be twice higher if a short-time atmosphere of CO was applied to the initial stage of reaction (2) (entry 5). On the other hand, if reaction

(2) was exclusively performed under CO atmosphere (entry 6), the resulting yield of **1** decreased to an analogous value as that obtained in reactions under N<sub>2</sub> atmosphere with the sole source of CO being the Pd<sub>10</sub> cluster (6) (compare entry 4 with entry 6). Thus, the *short-time* exposure to a CO atmosphere was found to avoid to a considerable extent the undesirable *competitive reaction* between Pd<sub>2</sub>dba<sub>3</sub> and CO with formation of Pd black and simultaneously to support the formation of **1** in reaction (2).

An attempt (entry 7) to use the mononuclear PdI<sub>2</sub>(PEt<sub>3</sub>)<sub>2</sub> complex (8) instead of binuclear PdI<sub>4</sub>(PEt<sub>3</sub>)<sub>2</sub> complex (7), in the absence of Pd<sub>10</sub>(CO)<sub>12</sub>(PEt<sub>3</sub>)<sub>6</sub> (6) gave only a small yield of **1** in reaction (3) mainly due to the decomposition of Pd<sub>2</sub>dba<sub>3</sub> to Pd black in the presence of CO:

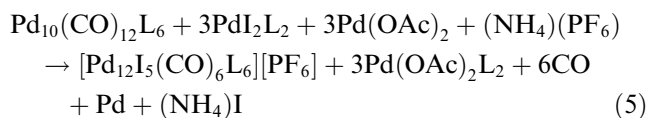


We found that the elimination of Pd<sub>2</sub>dba<sub>3</sub> from the starting reagents by replacement with Pd(OAc)<sub>2</sub> decreased the amount of Pd black and gave good yields of **1** (entry 8) in accordance with the idealized stoichiometry of the following reaction:



Reaction (4) implies the formation of PdI<sub>2</sub>L<sub>2</sub> (8) and Pd black, both of which were undesired products obtained from either direct iodination or conproportionation reactions.

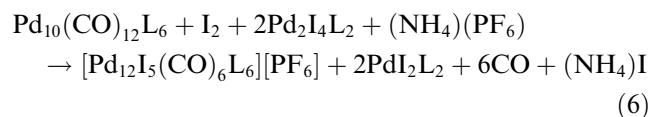
Entry 9 in Table 2 reveals that **1** can also be isolated from reactions of 6 with mononuclear PdI<sub>2</sub>L<sub>2</sub> (8). In this case, the rate of reaction was observed to be much slower compared with the rates of reactions (2) and (4), and needed one day instead of 1 h for completion. Furthermore, the rate of reaction and yield of **1** were found to be much higher upon the addition of Pd(OAc)<sub>2</sub> in the idealized stoichiometry of the following reaction (entry 10 versus entry 9):



Reactions of 6 and the PdI<sub>2</sub>L<sub>2</sub> complex (8), carried out with or without Pd(OAc)<sub>2</sub> (entry 10 versus entry 9), gave rise to the formation of a very unstable product, which was not characterized. In order to avoid contamination of **1** by this product and by products of its decomposition, recrystallization of **1** from THF/hexane solutions was effectively twice performed.

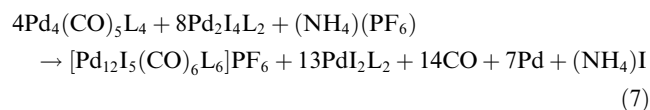
The above isolation of **1** from reactions of 6 via oxidation either with I<sub>2</sub> (entry 3) or from conproportiona-

tion with Pd<sub>2</sub>I<sub>4</sub>L<sub>2</sub> (7) (entry 4) raised the question as to whether both synthetic approaches could be combined, as shown (entry 11) in the idealized stoichiometry of the following reaction:



Though reaction (6), and likewise reaction (4), implies the formation of PdI<sub>2</sub>L<sub>2</sub> (8), the yields of **1** in these reactions are less than those from only the conproportionation reaction (2) (compare entries 11 and 12 versus entries 4–6). The yield of 110% for PdI<sub>2</sub>L<sub>2</sub> (8) (based only upon Pd<sub>2</sub>I<sub>4</sub>L<sub>2</sub> (7)) from reaction (6) performed under CO (entry 12) clearly indicates that its formation results from *both* palladium precursors Pd<sub>10</sub>(CO)<sub>12</sub>L<sub>6</sub> (6) and Pd<sub>2</sub>I<sub>4</sub>L<sub>2</sub> (7).

The use (entry 13) of Pd<sub>4</sub>(CO)<sub>5</sub>L<sub>4</sub> instead of Pd<sub>10</sub>(CO)<sub>12</sub>L<sub>6</sub> (6) in accordance with the idealized stoichiometry of reaction (7) afforded a 3–5 times lower yield of **1** than those found in reactions (2) and (4) (compare entry 13 versus entries 4–6, 8):



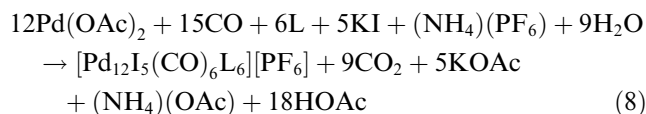
This observation is of particular interest, because clearly it indicates that even though **1** may be formally constructed from *three butterfly Pd<sub>4</sub> subunits joined by iodides* (see Fig. 1), a direct synthetic pathway involving this idealized condensation (of three butterfly Pd<sub>4</sub> cores) *in the presence of triethylphosphine and iodide* did not give rise to a higher yield.<sup>3</sup> In fact, this systematic investigation established that the highest yields of **1** were obtained from conproportionation reactions of Pd<sub>10</sub>(CO)<sub>12</sub>L<sub>6</sub> (6) with Pd<sub>2</sub>I<sub>4</sub>L<sub>2</sub> (7) in the presence of either Pd<sub>2</sub>dba<sub>3</sub> (entries 4–6) or Pd(OAc)<sub>2</sub> (entries 8 and 10).

### 2.3.4. Reduction of Pd(OAc)<sub>2</sub> by CO in presence of KI, PEt<sub>3</sub>, and (NH<sub>4</sub>)(PF<sub>6</sub>)

This synthetic pathway could conceivably have an obvious advantage upon comparison with the previous synthetic routes (presented above), because it does not require the synthesis of either the Pd<sub>10</sub> cluster (6) or other palladium clusters. However, in complete contrast to the previous preparation of triphenylphosphine Pd<sub>4</sub>I<sub>2</sub>(CO)<sub>3</sub>(PPh<sub>3</sub>)<sub>4</sub> in 80% yield by reduction of Pd(OAc)<sub>2</sub> with CO in the presence of iodide and PPh<sub>3</sub>

<sup>3</sup> Although a high yield of Pd<sub>12</sub>(CO)<sub>12</sub>(PPh<sub>3</sub>)<sub>6</sub> (5) obtained from condensation of Pd<sub>4</sub>(CO)<sub>5</sub>(PPh<sub>3</sub>)<sub>6</sub> [6a,6b] in the presence of oxygen (see [14b] and note added in proof in [12]) may be considered as a structure-to-synthesis appraisal, this approach does not necessarily have “cure-all” character.

[5a], **1** was isolated in very small quantity from the idealized stoichiometry of the following reaction (entry 14):



2.4. *Synthesis and characterization of the corresponding bromide analogue,  $[\text{Pd}_{12}(\mu_3\text{-Br})_2(\mu_4\text{-Br})_3(\mu_2\text{-CO})_6\text{L}_6]^+$  monocation (**9**) ( $\text{L} = \text{PEt}_3$ ;  $[\text{PF}_6]^-$  salt) from conproportionation reaction*

On the basis of the methodology utilized to prepare **1** from the conproportionation reaction (4), a similar reaction in THF of  $\text{Pd}_{10}(\text{CO})_{12}\text{L}_6$  with *trans*- $\text{Pd}_2(\mu_2\text{-Br})_2\text{Br}_2\text{L}_2$  in the presence of  $\text{Pd}(\text{OAc})_2$  and  $(\text{NH}_4)(\text{PF}_6)$  was carried out. A small quantity (<5%) of black-violet crystals, which readily transformed into oil, was isolated together with two square-planar palladium(II) bromide co-products, *trans*- $\text{PdBr}_2\text{L}_2$  (54%) and *cis*- $\text{PdBr}_2\text{L}_2$  (11%). The unambiguous formulation of **9** as the bromide analogue of **1** is based upon IR and  $^{31}\text{P}\{^1\text{H}\}$  NMR measurements which revealed virtually identical spectroscopic values: IR spectrum  $\nu(\text{CO})$ : THF solution, 1824 (s)  $\text{cm}^{-1}$ ;  $^{31}\text{P}\{^1\text{H}\}$  NMR spectrum,  $\text{CDCl}_3$  ( $\text{N}_2$ ), (121 MHz):  $\delta = 10.0$  ppm (s),  $-145$  ppm (septet). Particularly noteworthy is that the reflected/transmitted colors of a THF or  $\text{CDCl}_3$  solution of the black-violet crystals of **9** are the same as those of **1**: namely, black in reflected light, and violet in transmitted light. Both *trans*- and *cis*- $\text{PdBr}_2\text{L}_2$  co-products were identified from their  $^{31}\text{P}\{^1\text{H}\}$  and  $^{13}\text{C}\{^1\text{H}\}$  NMR spectra; yields are based upon the  $\text{Pd}_2\text{Br}_4\text{L}_2$  precursor ( $\text{L} = \text{PEt}_3$ ).

2.5. *Attempted syntheses of mixed Pd–Pt analogues of **1** or of other Pd–Pt clusters*

Cross mixed-metal conproportionation reactions were carried out. Analogous to the corresponding homopalladium reaction in entry 10, the first one (a) involved the reaction of palladium(0)  $\text{Pd}_{10}(\text{CO})_{12}\text{L}_6$  with platinum(II)  $\text{PtI}_2\text{L}_2$  in the presence of  $\text{Pd}(\text{OAc})_2$  and  $(\text{NH}_4)(\text{PF}_6)$ . The second one (b) involved the reaction of platinum(0)  $\text{Pt}_5(\text{CO})_6(\text{PEt}_3)_4$  with palladium(II)  $\text{Pd}_2\text{I}_4\text{L}_2$  in the presence of  $(\text{NH}_4)(\text{PF}_6)$ .

Neither reaction afforded heterometallic Pd–Pt clusters, but instead gave the following identified products with estimated yields (in parentheses): **1** (57%) and **8** (3%) for reaction (a), and **1** (4%), **8** (6%),  $\text{Pt}_2\text{I}_4\text{L}_2$  (11%), and *trans*- $\text{PtI}_2\text{L}_2$  (54%) for reaction (b). The actual transfer in reaction (a) of the iodide ligands from the platinum(II)  $\text{PtI}_2\text{L}_2$  to **1** with each Pd possessing a formal oxidation state of +0.5 indicates a relatively strong binding of the  $\mu_3\text{-I}$  and  $\mu_4\text{-I}$  ligands to the  $\text{Pd}_{12}$  polyhedron in **1**. Other chemical evidence of the

bridging iodide ligands being strongly linked to the  $\text{Pd}_{12}$  polyhedron in **1** is that we did not observe either their elimination as AgI upon treatment of solutions of **1** (in THF,  $\text{Me}_2\text{CO}$ , or MeCN) with  $\text{Ag}(\text{OAc})$  or any signs (within a reasonable time) of reaction between **1** and  $\text{TiCo}(\text{CO})_4$ . Furthermore, whereas palladium carbonyl/phosphine clusters and their known halide derivatives are generally sensitive to air, it was found that **1** in dried form is stable under air for at least one month.

2.6. *Spectroscopic characterization of **1***

An IR spectrum of **1** in THF solution exhibited one strong carbonyl band at  $1826\text{ cm}^{-1}$ , whereas an IR spectrum of **1** in nujol displayed one broadened strong carbonyl band at  $1810\text{ cm}^{-1}$ . These spectra suggest the presence of just one type of bridging carbonyl ligand.

$^{31}\text{P}\{^1\text{H}\}$  NMR spectra of **1** in  $\text{CDCl}_3$  solution under  $\text{N}_2$  exhibited one signal at 7.4 ppm indicative of six equivalent phosphorus nuclei. A NMR  $^{13}\text{C}\{^1\text{H}\}$  spectrum of a  $\text{CDCl}_3$  solution of crystals of **1** showed strong signals of methylene and methyl carbon nuclei from the phosphorus-attached ethyl substituents at 18.1 and 8.7 ppm, respectively; a low-field signal at 215.7 ppm was attributed to the  $^{13}\text{C}$  nuclei of six carbonyl ligands, and two equal weak signals at 68.2 and 25.8 ppm were ascribed to nuclei of the original crystal-solvated THF molecules. The signal at 215.7 ppm was readily assigned to the carbonyl  $^{13}\text{C}$  nuclei on the basis of its relative intensity and chemical shift value. The assignment of the two weak signals to THF was substantiated from a control  $^{13}\text{C}\{^1\text{H}\}$  NMR spectrum of THF (recorded at the same conditions) which consisted of singlets at 67.8 ( $\text{CH}_2\text{-O}$ ) and 25.5 ppm ( $\text{C-CH}_2\text{-CH}_2\text{-C}$ ). Noteworthy is that the methylene  $^{13}\text{C}$  signals in **1** consisted of an unresolved multiplet (with the appearance of a distorted triplet) which could only arise from  $^4J(\text{P,P})$  coupling [16]. In the absence of  $J(\text{P,P})$  interactions, it should be a doublet due to only  $^1J(\text{C,P})$  coupling (i.e., as was observed for a first-order spectrum of **7**), whereas for the presence only one type of  $J(\text{P,P})$  coupling – a triplet (i.e., as was observed for a second-order spectrum of **8** [17a] and for a number of related compounds with only  $^2J(\text{P,P})$  interactions between phosphorus atoms [17]). The observation of the above-mentioned multiplet for the  $^{13}\text{C}$  methylene signals in **1** indicates two possible types of  $^4J(\text{P,P})$  coupling realized through both kinds of  $\text{PPd}(\text{cap})\text{Pd}(\text{oc})_2\text{Pd}(\text{cap})\text{P}$  butterfly fragments of **1**: namely, the three symmetry-equivalent ( $\mu_4\text{-I}$ )-occupied ones and the three symmetry-equivalent unoccupied ones with two  $\mu_2\text{-CO}$  ligands spanning two of the four wingtip-hinge  $\text{Pd}(\text{cap})\text{-Pd}(\text{oc})$  edges. The  $^4J(\text{P,P})$  coupling in the latter butterfly-shaped  $\text{PPd}(\text{cap})(\mu_2\text{-CO})\text{Pd}(\text{oc})_2(\mu_2\text{-CO})\text{Pd}(\text{cap})\text{P}$  fragment may include a  $^3J(\text{P,P})$  component due to relatively weak, but direct interaction

between the two P-attached wingtip Pd(cap) atoms separated by 3.33 Å.

A NMR  $^1\text{H}$  spectrum of a  $\text{CDCl}_3$  solution of crystals of **1** displayed a doublet of triplets (dt) at 1.13 ppm ( $-\text{CH}_3$ ) and a multiplet at 1.94 ppm ( $-\text{CH}_2-\text{P}$ ), which could be either a sextet or octet. Reliable definition of its multiplicity is virtually impossible due to overlapping of higher field edge of this signal with the complex pattern of signals from the methylene protons,  $\text{C}-\text{CH}_2-\text{CH}_2-\text{C}$ , of the THF molecule at 1.85 ppm. In any event, the methylene proton signal at 1.94 ppm could not be explained in terms of a first-order spectrum. In contrast to this signal, the methyl proton signal at 1.13 corresponds to a first-order spectrum with only  $^3J(\text{H,H})$  and  $^3J(\text{H,P})$  splitting. As mentioned above, one group of proton signals of the THF molecule was observed at 1.85 ppm, while the second one from the two  $\text{CH}_2-\text{O}$  fragments was displayed at 3.75 ppm with the specific symmetrical pattern precisely corresponding to that at 3.73 ppm for the THF control spectrum per se. Comparison of its integral intensity with that of the dt signal of  $\text{CH}_3$  and the overlapped signals at 1.94 ppm of  $\text{CH}_2-\text{P}$  gave virtually the same ratios of 1/37 and 1/38, respectively, which correspond to the 1/THF ratio of 1/0.4 for crystals of **1** grown from THF/hexane. (A small contribution of THF into the integral intensity of signals from  $\text{CH}_2-\text{P}$  at 1.94 ppm was taken into account by subtraction of the integral intensity of signals at 3.75 ppm, which is equal to the overlapped THF component.)

The determined chemical shifts in the NMR  $^1\text{H}$  spectrum of **7** and NMR  $^{31}\text{P}\{^1\text{H}\}$ ,  $^{13}\text{C}\{^1\text{H}\}$  and  $^1\text{H}$  spectra of **8** are in good agreement with ones reported previously [17a].

### 2.7. Comparative structural/bonding analysis of the co-products **7** and **8**

The molecular square-planar palladium(II) structures of *trans*- $\text{Pd}_2(\mu_2-\text{I})_2\text{I}_2(\text{PEt}_3)_2$  (**7**) and *trans*- $\text{PdI}_2(\text{PEt}_3)_2$  (**8**) were established unequivocally from low-temperature CCD X-ray crystallography. Fig. 3(a) and (b) displays their geometries (without Et substituents) with atom-labeling; selected bond lengths and bond angles for both the iodide-bridged dimeric **7** and monomeric **8** are listed in Table 3 along with molecular parameters which agree extremely well with those given for other phosphine iodide analogues [18].

A comparison of *trans*- $\text{Pd}_2(\mu_2-\text{I})_2\text{I}_2(\text{PEt}_3)_2$  (**7**) with the tri(*n*-butyl)phosphine analogue [18a] and diphenylvinylphosphine iodide analogue [18b] reveals that the bridging Pd–I(b) bonds (range 2.660–2.685(1) Å) *trans* to the phosphine ligands are considerably longer than the Pd–I(b) bonds (range 2.593(2)–2.608(1) Å) *trans* to the terminal I(t) iodides and the Pd–I(t) bonds (range 2.581(2)–2.595(1) Å). The resulting asymmetric  $\text{Pd}_2\text{I}(\text{b})_2$  rhombus of each complex possesses distinctly different

Pd–I(b)–Pd' bond angles (range 94.61(2)–95.68(5)°) and I(b)–Pd–I(b') bond angles (range 84.32(5)–85.39(2)°). The Pd–P bonds (range 2.248–2.263(1) Å) are likewise essentially equivalent.

Table 3 discloses that the corresponding molecular parameters determined at 100 K for the two centrosymmetric half-molecules A and B of *trans*- $\text{PdI}_2(\text{PEt}_3)_2$  (**8**) are virtually identical with those previously determined [18c] for **8** at 293(2) K, even though the unit cell volume and corresponding monoclinic lattice parameters are significantly different (with the corresponding low-temperature values being expectedly smaller than those at room-temperature).<sup>4</sup> Table 3 also shows that the corresponding molecular parameters are in remarkably close agreement with those of the triphenylphosphine analogue (both unsolvated [18d] and chloroform solvated [18e]). Noteworthy is that the Pd–I(t) distances (range 2.598(1)–2.610(1) Å) for these *trans*- $\text{PdI}_2(\text{PR}_3)_2$  complexes compare favorably (within 0.02 Å) with both the terminal Pd–I(t) and bridging Pd–I(b) distances whose bonds are *trans* to the terminal I(t) bonds for the *trans*- $\text{Pd}_2(\mu_2-\text{I})_2\text{I}_2(\text{PR}_3)_2$  dimers. The markedly longer mean distance of ca. 0.08 Å for the bridging Pd–I(b) bonds *trans* to the phosphine ligands in the dimers may be attributed to the *trans* influence [19]. The other salient structural feature illustrated in Table 3 is that the two symmetry-equivalent terminal Pd–P bonds in the *trans*- $\text{Pd}_2(\mu_2-\text{I})_2\text{I}_2(\text{PR}_3)_2$  dimers are approximately 0.10 Å shorter than those in the *trans*- $\text{PdI}_2(\text{PR}_3)_2$  monomers; this distinct bond-length variation may likewise be ascribed to an electronic effect primarily involving the *trans* ligand in a localized square-planar palladium(II) environment. This highly significant difference is in accordance with X-ray crystallographic bond-length observations which led to the proposal 30 years ago that “a metal-phosphine bond was less stable *trans* to another phosphine than when *trans* to a halide” [19].

<sup>4</sup> The initial high-quality structural determination of *trans*- $\text{PdI}_2(\text{PEt}_3)_2$  (**8**) reported by Fehlhammer and co-workers [18c] in 2001 was based upon X-ray diffractometry data collected with Mo K $\alpha$  radiation at room-temperature (293(2) K). Crystal data include the following: monoclinic;  $P2_1/c$  with  $Z = 4$ ;  $a = 17.726(4)$  Å,  $b = 8.116(2)$  Å,  $c = 15.569(6)$  Å,  $\beta = 113.35(3)^\circ$ .  $V = 2056.4(10)$  Å<sup>3</sup>. Corresponding crystal data collected at 100(2) K in our independent structural determination of *trans*- $\text{PdI}_2(\text{PEt}_3)_2$  (**8**) presented herein are:  $P2_1/c$  with  $Z = 4$ ;  $a = 17.688(2)$  Å,  $b = 7.899(1)$  Å,  $c = 15.543(2)$  Å,  $\beta = 114.48(1)^\circ$ .  $V = 1976.3(4)$  Å<sup>3</sup>. Both analogous structural refinements resulted in reasonably close agreement of final unweighted and weighted  $R$  indices: namely, unweighted  $R_1(F) = 0.035$  versus 0.025 [ $I > 2\sigma(I)$ ] and weighted  $wR_2(F^2) = 0.102$  versus 0.067 (all data). We conclude that the significantly smaller volume difference of 80 Å<sup>3</sup> and smaller  $b$  lattice-length difference of 0.22 Å reported in our structural determination are primarily a consequence of our low-temperature data collection. Of prime interest is that the corresponding molecular parameters for the two structural determinations are amazingly alike (within 0.007 Å and 0.35°).

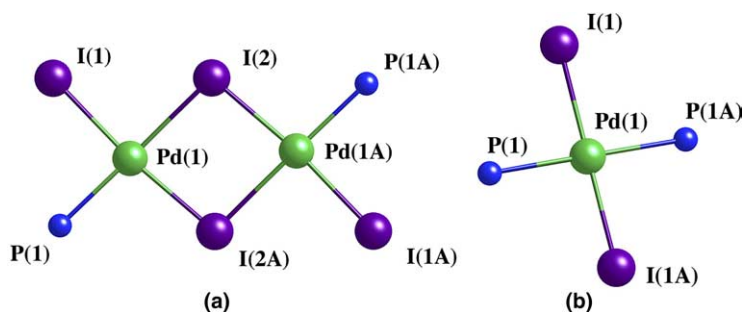


Fig. 3. Molecular square-planar palladium(II) geometries (without Et substituents) of: (a) dimeric *trans*-Pd<sub>2</sub>(μ<sub>2</sub>-I)<sub>2</sub>I<sub>2</sub>(PEt<sub>3</sub>)<sub>2</sub> (**7**); and (b) monomeric *trans*-PdI<sub>2</sub>(PEt<sub>3</sub>)<sub>2</sub> (**8**).

Table 3

Comparison of selected bond lengths (Å) and angles (°) for *trans*-Pd<sub>2</sub>(μ<sub>2</sub>-I)<sub>2</sub>I<sub>2</sub>(PEt<sub>3</sub>)<sub>2</sub> (**7**) and *trans*-PdI<sub>2</sub>(PEt<sub>3</sub>)<sub>2</sub> (**8**) with several known analogues<sup>a</sup>

Complex <sup>a</sup>	Ref.	Pd(1)–I(1)	Pd(1)–I(2)	Pd(1)–I(2A)	Pd(1)–P(1)	P(1)–Pd(1)–I(1)	I(2)–Pd(1)–I(2A)	Pd(1)–I(2)–Pd(1A)
<i>trans</i> -Pd <sub>2</sub> I <sub>4</sub> (PR <sub>3</sub> ) <sub>2</sub> , R = Et ( <b>7</b> ) <sup>b</sup>	present work	2.595(1)	2.685(1)	2.608(1)	2.263(1)	90.19(3)	85.39(2)	94.61(2)
<i>trans</i> -Pd <sub>2</sub> I <sub>4</sub> (PR <sub>3</sub> ) <sub>2</sub> , R = <i>n</i> -Bu <sup>c</sup>	[18a]	2.581(2)	2.666(2)	2.593(2)	2.256(4)	90.0(1)	84.32(5)	95.68(5)
<i>trans</i> -Pd <sub>2</sub> I <sub>4</sub> (PR <sub>3</sub> ) <sub>2</sub> , R <sub>3</sub> = Ph <sub>2</sub> (CHCH <sub>2</sub> ) <sup>d</sup>	[18b]	2.583	2.660	2.593	2.248	90.3	84.8	94.8
<i>trans</i> -PdI <sub>2</sub> (PEt <sub>3</sub> ) <sub>2</sub> ( <b>8</b> ) <sup>e</sup>	present work							
Molecule A		2.608(1)			2.346(1)	87.08(2), 92.92(2)		
Molecule B		2.610(1)			2.343(1)	87.15(2), 92.85(2)		
<i>trans</i> -PdI <sub>2</sub> (PEt <sub>3</sub> ) <sub>2</sub> <sup>f</sup>	[18c]							
Molecule A		2.602(1)			2.346(2)	87.25(5), 92.75(5)		
Molecule B		2.601(1)			2.342(2)	87.45(5), 92.55(5)		
<i>trans</i> -PdI <sub>2</sub> (PPh <sub>3</sub> ) <sub>2</sub> <sup>g</sup>	[18d]	2.598(1)			2.350(1)	88.45(3), 91.55(3)		
<i>trans</i> -PdI <sub>2</sub> (PPh <sub>3</sub> ) <sub>2</sub> · CHCl <sub>3</sub> <sup>h</sup>	[18e]	2.603(1)			2.343(2)	87.56(5), 92.32(5)		

<sup>a</sup> Atom-labeling for both *trans*-Pd<sub>2</sub>(μ<sub>2</sub>-I)<sub>2</sub>I<sub>2</sub>(PEt<sub>3</sub>)<sub>2</sub> (**7**) and *trans*-PdI<sub>2</sub>(PEt<sub>3</sub>)<sub>2</sub> (**8**) is given in Fig. 3.

<sup>b</sup> CCD X-ray data taken at 100(2) K; one crystallographically independent half-molecule with C<sub>i</sub> (1) site symmetry.

<sup>c</sup> X-ray data taken at room temperature; one crystallographically independent half-molecule with C<sub>i</sub> (1) site symmetry.

<sup>d</sup> X-ray data taken at 290 K; two crystallographically independent molecules with C<sub>1</sub> (1) site symmetry. The mean of four individual connectivities is given for each different (bond/angle)-type.

<sup>e</sup> CCD X-ray data taken at 100(2) K; two crystallographically independent half-molecules A and B with C<sub>i</sub> (1) site symmetry.

<sup>f</sup> X-ray data taken at 293(2) K; two crystallographically independent half-molecules A and B with C<sub>i</sub> (1) site symmetry.

<sup>g</sup> X-ray data taken at 160(2) K; one crystallographically independent half-molecule with C<sub>i</sub> (1) site symmetry.

<sup>h</sup> X-ray data taken at 300 K; one crystallographically independent half-molecule with C<sub>2</sub> (2) site symmetry.

### 3. Experimental

#### 3.1. Materials and methods

Reactions were carried out via standard Schlenk techniques on a preparative vacuum line under nitrogen atmosphere. All solvents were deoxygenated prior to use by the passing of N<sub>2</sub> through them for at least 20 min at room temperature. [Pd<sub>6</sub>Tl(μ<sub>2</sub>-CO)<sub>6</sub>L<sub>6</sub>][PF<sub>6</sub>]<sub>2</sub> (**2**), [Pd<sub>12</sub>Tl<sub>2</sub>(CO)<sub>9</sub>L<sub>9</sub>][PF<sub>6</sub>]<sub>2</sub> (**3**), and Pd<sub>4</sub>(CO)<sub>5</sub>L<sub>4</sub> were synthesized by known methods [9,10,20], and Pd<sub>10</sub>(CO)<sub>12</sub>L<sub>6</sub> (**6**) was prepared as described for

Pd<sub>10</sub>(CO)<sub>12</sub>(PBU<sub>3</sub>)<sub>6</sub> [6e] and was purified via recrystallization from C<sub>6</sub>H<sub>6</sub>/heptane. For preparation of *trans*-Pd<sub>2</sub>I<sub>4</sub>(PEt<sub>3</sub>)<sub>2</sub> (**7**) and *trans*-PdI<sub>2</sub>(PEt<sub>3</sub>)<sub>2</sub> (**8**) we used the published procedure [21] but with PdCl<sub>2</sub> instead of hydrated Na<sub>2</sub>PdCl<sub>4</sub>. Other chemicals were purchased and used without additional purification.

<sup>31</sup>P{<sup>1</sup>H}, <sup>13</sup>C{<sup>1</sup>H} and <sup>1</sup>H NMR spectra were obtained for CDCl<sub>3</sub> solutions under N<sub>2</sub> atmosphere on a Bruker AM-300 spectrometer. <sup>31</sup>P{<sup>1</sup>H} spectra were referenced to 85% H<sub>3</sub>PO<sub>4</sub> in D<sub>2</sub>O as an external standard. <sup>13</sup>C chemical shifts were referenced to TMS via the <sup>13</sup>C signal of the solvent CDCl<sub>3</sub> at 77.23 ppm. <sup>1</sup>H chemical

shifts were referenced to internal TMS. Each NMR sample was prepared by use of a nitrogen/vacuum line. Infrared spectra were recorded on a Mattson Polaris FT-IR spectrometer by use of a nitrogen-purged CaF<sub>2</sub> cell. Nujol suspensions were prepared under nitrogen as well.

Yields of crystals **1**, **5**, **6** were defined by their mechanical separation under a microscope and/or from an NMR <sup>31</sup>P{<sup>1</sup>H} technique by use of an inner standard, as described below. An integral intensity of a <sup>31</sup>P{<sup>1</sup>H} signal of one of the compounds (e.g., **1**, **7**, or **8**) in an initial NMR spectrum of a mixture of two or three crystalline species was used as a reference. Then a weighed amount of the crystals of one of the defining compounds was added into the NMR tube. The resulting spectrum was analyzed via the increased intensity of the signal of the added compound versus the unchanged reference signal; this method provided a direct way to calculate the cluster's yield. The signals at 7.4 ppm for **1** and 7.6 ppm for **8** were sufficiently resolved due to their narrow lines.

### 3.2. Synthesis of [Pd<sub>12</sub>(μ<sub>3</sub>-I)<sub>2</sub>(μ<sub>4</sub>-I)<sub>3</sub>(μ<sub>2</sub>-CO)<sub>6</sub>L<sub>6</sub>]<sup>+</sup>, **1**, as [PF<sub>6</sub>]<sup>-</sup> salt (L = PEt<sub>3</sub>)

#### 3.2.1. Direct iodination of (μ<sub>6</sub>-TI)[Pd<sub>3</sub>(CO)<sub>3</sub>L<sub>3</sub>]<sub>2</sub><sup>+</sup> sandwich ([PF<sub>6</sub>]<sup>-</sup> salt)

A solution of I<sub>2</sub> (30 mg; 0.118 mmol) in 4 mL of THF was added dropwise under stirring to a solution of [TIPd<sub>6</sub>(CO)<sub>6</sub>L<sub>6</sub>]<sup>+</sup>PF<sub>6</sub><sup>-</sup> (0.100 g; 0.0536 mmol) in 3 mL of THF. The solution color immediately changed to red and then to brown-red. An IR spectrum of the reaction solution taken after 30 min showed characteristic carbonyl bands of **1**, 1827 (m) cm<sup>-1</sup>; **3**, 1873 (m), 1845 (m) cm<sup>-1</sup>; and an unassigned band at 1899 (m) cm<sup>-1</sup>. After 1 h of stirring, an additional amount of I<sub>2</sub> (31 mg; 0.122 mmol) was added, which resulted in an immediate formation of black precipitate. After 2 h an IR spectrum of the reaction solution displayed only one strong carbonyl band at 1826 cm<sup>-1</sup> due to **1**. The solution was filtrated from Pd black, 17 mg; subsequent crystallization from the THF solution in the presence of hexane gave 4 mg of black-violet crystals of [Pd<sub>12</sub>(μ<sub>3</sub>-I)<sub>2</sub>(μ<sub>4</sub>-I)<sub>3</sub>(μ<sub>2</sub>-CO)<sub>6</sub>L<sub>6</sub>]<sup>+</sup>PF<sub>6</sub><sup>-</sup> (**5**), 50 mg of *trans*-Pd<sub>2</sub>I<sub>4</sub>L<sub>2</sub>, **7** (32%) and 32 mg of *trans*-PdI<sub>2</sub>L<sub>2</sub>, **8** (17%). These estimated yields were defined by the previously described NMR technique (Table 2, entry 1).

Reactions of **3** and **6** with iodine were carried out analogously (Table 2, entries 2 and 3). From these reactions single crystals of **1**, **7**, and **8** were separated mechanically and used for multinuclear NMR and X-ray diffraction studies. Particularly noteworthy is that there were three types of black-violet single crystals of **1**: namely, blocks, needles and hexagonal hollow tubes;

but X-ray diffraction measurements revealed that all of them possessed the same unit cell. One block crystal of size 0.41 × 0.20 × 0.17 mm<sup>3</sup> was used for the CCD X-ray data collection.

IR spectra of **1**, ν(CO): nujol, 1810 (s) cm<sup>-1</sup>; THF solution, 1826 (s) cm<sup>-1</sup>.

<sup>31</sup>P{<sup>1</sup>H} NMR spectrum of **1** (121 MHz): δ = 7.4 ppm (s), -145.2 ppm (septet, <sup>1</sup>J(P,F) = 715 Hz). <sup>13</sup>C{<sup>1</sup>H} NMR spectrum of **1** (75.4 MHz): δ = 215.7 ppm (s, 6C, CO), 68.2 ppm (s, ~0.8C, CH<sub>2</sub>-O), 25.8 ppm (s, ~0.8C, C-CH<sub>2</sub>-CH<sub>2</sub>-C), 18.1 ppm (complex multiplet with three main signals at 18.242, 18.105 and 17.999 ppm, 18C, CH<sub>2</sub>-P), 8.7 ppm (s, 18C, CH<sub>3</sub>). <sup>1</sup>H NMR spectrum of **1** (300 MHz): δ = 3.75 ppm (m, ~1.6H, CH<sub>2</sub>-O), 1.94 ppm (m, 36H, CH<sub>2</sub>-P), 1.85 ppm (m, ~1.6H, C-CH<sub>2</sub>-CH<sub>2</sub>-C), 1.13 ppm (dt, 54H, CH<sub>3</sub>, <sup>3</sup>J(H,H) = 7.7 Hz; <sup>3</sup>J(H,P) = 15.7 Hz). <sup>31</sup>P{<sup>1</sup>H} NMR spectrum of **7** (121 MHz): δ = 42.4 ppm (s). <sup>13</sup>C{<sup>1</sup>H} NMR spectrum of **7** (75.4 MHz): δ = 21.5 ppm (d, 6C, CH<sub>2</sub>, <sup>1</sup>J(C,P) = 32.8 Hz), 9.2 ppm (s, 6C, CH<sub>3</sub>). <sup>1</sup>H NMR spectrum of **7** (300 MHz): δ = 2.23 ppm (dq, 12H, CH<sub>2</sub>, <sup>3</sup>J(H,H) = 7.6 Hz, <sup>2</sup>J(H,P) = 10.4 Hz), 1.22 ppm (dt, 18H, CH<sub>3</sub>, <sup>3</sup>J(H,H) = 7.6 Hz, <sup>3</sup>J(H,P) = 18.2 Hz). <sup>31</sup>P{<sup>1</sup>H} NMR spectrum of **8** (121 MHz): δ = 7.6 ppm (s). <sup>13</sup>C{<sup>1</sup>H} NMR spectrum of **8** (75.4 MHz): δ = 20.2 ppm (t, 6C, CH<sub>2</sub>, <sup>1</sup>J(C,P) + <sup>3</sup>J(C,P) = 29.9 Hz), 9.1 ppm (s, 6C, CH<sub>3</sub>). <sup>1</sup>H NMR spectrum of **8** (300 MHz): δ = 2.28 ppm (qt, 12H, CH<sub>2</sub>, <sup>3</sup>J(H,H) = 7.8 Hz, <sup>2</sup>J(H,P) + <sup>4</sup>J(H,P) = 6.6 Hz), 1.11 ppm (tt, 18H, CH<sub>3</sub>, <sup>3</sup>J(H,H) = 7.8 Hz, <sup>3</sup>J(H,P) + <sup>5</sup>J(H,P) = 33.6 Hz).

#### 3.2.2. Conproportionation reactions

The following typical reaction is a detailed description of entry **8** (Table 2). A mixture of Pd<sub>10</sub>(CO)<sub>12</sub>L<sub>6</sub> (0.100 g; 0.0474 mmol), *trans*-Pd<sub>2</sub>I<sub>4</sub>L<sub>2</sub> (91 mg; 0.0951 mmol), Pd(OAc)<sub>2</sub> (10.6 mg; 0.0472 mmol), and (NH<sub>4</sub>)(PF<sub>6</sub>) (15.5 mg; 0.0951 mmol) was stirred in 10 mL of THF. The solution color changed from red to black-violet within 10–15 min. After 3 h the solvent was evaporated via N<sub>2</sub> flow. Extraction of the residue with Et<sub>2</sub>O resulted in the separation of 60 mg of yellow crystals of **8**. The remaining residue was washed with water and dried via vacuum under liquid N<sub>2</sub>, after which **1** was extracted from the residue by use of 15 mL of THF; subsequent addition of ca. 12 mL of hexane and keeping of the solution overnight at -20 °C gave 63 mg (54%) of black-violet crystals of **1**. The final residue was Pd black, 21 mg. Both crystalline compounds **1**[PF<sub>6</sub>]<sup>-</sup> and **8** were characterized spectroscopically (Table 2, entry 8).

All other conproportionation reactions were performed either analogously or under specific conditions discussed in Section 2 and mentioned in the footnotes of Table 2.

### 3.2.3. Reduction of $\text{Pd}(\text{OAc})_2$ by CO in the presence of KI, $\text{PEt}_3$ and $(\text{NH}_4)(\text{PF}_6)$

This reaction is a detailed description of entry 14 (Table 2). To a solution of  $\text{Pd}(\text{OAc})_2$  (0.224 g; 1.00 mmol) in 12 mL of acetone the following reagents were added consecutively under stirring: HOAc (3 mL),  $(\text{NH}_4)(\text{PF}_6)$  (55 mg; 0.34 mmol),  $\text{PEt}_3$  (73  $\mu\text{L}$ ; 0.50 mmol), KI (70 mg; 0.42 mmol) and  $\text{H}_2\text{O}$  (3 mL). After 1 day of stirring under CO atmosphere, 15 mL of  $\text{H}_2\text{O}$  were added. The resulting back precipitate was filtered, washed with  $\text{H}_2\text{O}$ , extracted with 90% EtOH, and then with  $\text{Et}_2\text{O}$ . The ethanol extract gave 4 mg of **1** (1.6%) and 18 mg of **8**. Additionally, 56 mg of **8** were obtained from the  $\text{Et}_2\text{O}$  extract, corresponding to a total yield of 12%. Extraction of the remaining residue with THF led to the formation of an extremely unstable brown solution. The final residue, 70 mg, was Pd black.

### 3.3. X-ray crystallographic determinations

#### 3.3.1. General procedures

X-ray data for crystals of  $[\mathbf{1}]\text{PF}_6$ , **7**, and **8** were collected at 100(2) K via a Bruker SMART CCD-1000 area detector diffractometer with graphite-monochromated Mo  $\text{K}\alpha$  radiation ( $\lambda = 0.71073 \text{ \AA}$ ) from a sealed-tube generator. The crystal structures were determined from direct methods. Full-matrix least-squares refinements (based on  $F^2$ ) were carried out with SHELXTL [22].

CCDC reference numbers 246935 (**1**), 246936 (**7**), and 246937 (**8**).

#### 3.3.2. $[\text{Pd}_{12}\text{I}_5(\text{CO})_6(\text{PEt}_3)_6][\text{PF}_6]$

$M = 2933.2$ ,  $P\bar{3}1C$ ,  $a = b = 17.4050(7) \text{ \AA}$ ,  $c = 15.8014(9) \text{ \AA}$ ,  $\alpha = \beta = 90^\circ$ ,  $\gamma = 120^\circ$ ,  $V = 4145.5(3) \text{ \AA}^3$ ,  $Z = 2$ ;  $F(000) = 2732$ ;  $D_{\text{calc}} = 2.350 \text{ Mg} \cdot \text{m}^{-3}$ . 33490 reflections were obtained over  $5.40 \leq \theta \leq 52.72^\circ$ . Empirical absorption correction (SADABS) was applied [ $\mu(\text{Mo-K}\alpha) = 4.578 \text{ mm}^{-1}$ , maximum/minimum transmission, 0.5100/0.2555]. Refinement of 2836 independent merged reflections [ $R_{\text{int}} = 0.0350$ ] with 89 parameters (13 restraints) converged at  $wR_2(F^2) = 0.1772$  for all data;  $R_1(F) = 0.0511$  for  $I > 2\sigma(I)$ ; maximum/minimum residual electron density,  $1.47/-1.06 \text{ e} \cdot \text{\AA}^{-3}$ ; goodness-of-fit (on  $F^2$ ) = 1.127. Under  $P\bar{3}1c$  symmetry with  $Z = 2$ , the two monocations (**1**) and two  $[\text{PF}_6]^-$  anions each possess 32 site symmetry. The crystallographically independent unit of **1** consists of one Pd(oc) and one Pd(cap) in 12-fold general positions, one  $\mu_4\text{-I}$  on a horizontal twofold axis, one  $\mu_3\text{-I}$  on the threefold axis, and one carbonyl C and O atoms and six ethyl carbon atoms in 12-fold general positions; the independent part of the two anions has one P atom with 32 point symmetry and one F atom in 12-fold general positions. All non-hydrogen atoms, except for the ethyl carbon atoms, were refined anisotropically. Most carbon atoms of the ethyl groups showed multiple disorder, which did not model. Hydro-

gen atoms were included in structure factor calculations at idealized positions and were allowed to ride on attached carbon atoms with relative isotropic displacement coefficients. The displacement ellipsoids of the P and F atoms were elongated along the  $c$ -direction, thereby indicating dominant anisotropic thermal displacement along the threefold axis. The final difference map revealed around a 32 site two physically meaningful residual peaks, Q5 and Q8, which could be attributed either to O or C atoms of a solvated THF molecule disordered among six equivalent positions. This crystallographic assignment is completely consistent with a  $^1\text{H}$  NMR spectrum of single crystals dissolved in  $\text{CDCl}_3$ , which exhibited a proton resonance at 3.75 ppm characteristic of the  $-\text{CH}_2\text{-O-CH}_2-$  part of the  $\text{C}_4\text{H}_8\text{O}$  molecule. An estimated **1**/THF ratio of 1/0.4 (that roughly corresponds one-half of a solvated molecule) was found upon the comparison of the integral intensity for this signal with those for the methylene and methyl signals of the  $\text{PEt}_3$  ligands of **1**. Because approximately one-half of a solvated THF molecule in the independent unit disordered over six equivalent orientations would give rise to only 1/12th the normal electron density of C or O atoms at each atomic position, this presumed crystal disorder was not modeled.

#### 3.3.3. $\text{trans}-(\text{PEt}_3)_2\text{PdI}_4$

$M = 956.70$ ,  $P2_1/n$ ,  $a = 8.9860(12) \text{ \AA}$ ,  $b = 14.2391(19) \text{ \AA}$ ,  $c = 9.3548(13) \text{ \AA}$ ,  $\alpha = \gamma = 90^\circ$ ,  $\beta = 91.927(2)^\circ$ ,  $V = 1196.3(3) \text{ \AA}^3$ ,  $Z = 2$ ;  $F(000) = 872$ ;  $D_{\text{calc}} = 2.656 \text{ Mg} \cdot \text{m}^{-3}$ . 10869 reflections were obtained over  $5.22 \leq \theta \leq 56.62^\circ$ . Empirical absorption correction (SADABS) was applied [ $\mu(\text{Mo-K}\alpha) = 6.790 \text{ mm}^{-1}$ , maximum/minimum transmission, 0.3166/0.1720]. Refinement of 2945 independent merged reflections [ $R_{\text{int}} = 0.0302$ ] with 91 parameters (0 restraints) converged at  $wR_2(F^2) = 0.0678$  for all data;  $R_1(F) = 0.0262$  for  $I > 2\sigma(I)$ ; maximum/minimum residual electron density,  $1.200/-0.662 \text{ e} \cdot \text{\AA}^{-3}$ ; goodness-of-fit (on  $F^2$ ) = 0.942. Crystal size:  $0.40 \times 0.29 \times 0.22 \text{ mm}^3$ . All non-hydrogen atoms were refined anisotropically. Hydrogen atoms were included as described above. The  $\text{trans}-(\text{PEt}_3)_2\text{PdI}_4$  complex was also crystallized in the orthorhombic crystal system with  $a = 6.995(2) \text{ \AA}$ ,  $b = 14.272(3) \text{ \AA}$ ,  $c = 23.730(5) \text{ \AA}$ ,  $\alpha = \beta = \gamma = 90^\circ$ ,  $V = 2369.1(8) \text{ \AA}^3$ ,  $Z = 4$ .

#### 3.3.4. $\text{trans}-(\text{PEt}_3)_2\text{PdI}_2$

$M = 596.50$ ,  $P2_1/c$ ,  $a = 17.6876(19) \text{ \AA}$ ,  $b = 7.8987(8) \text{ \AA}$ ,  $c = 15.5429(17) \text{ \AA}$ ,  $\alpha = \gamma = 90^\circ$ ,  $\beta = 114.4770(10)^\circ$ ,  $V = 1976.3(4) \text{ \AA}^3$ ,  $Z = 4$ ;  $F(000) = 1136$ ;  $D_{\text{calc}} = 2.005 \text{ Mg} \cdot \text{m}^{-3}$ . 4872 reflections were obtained over  $2.52 \leq \theta \leq 56.56^\circ$ . Empirical absorption correction (SADABS) was applied [ $\mu(\text{Mo-K}\alpha) = 4.209 \text{ mm}^{-1}$ , maximum/minimum transmission, 0.4074/0.3050]. Refinement of 4872 independent merged reflections

[ $R_{\text{int}} = 0.0297$ ] with 163 parameters (0 restraints) converged at  $wR_2(F^2) = 0.0671$  for all data;  $R_1(F) = 0.0251$  for  $I > 2\sigma(I)$ ; maximum/minimum residual electron density,  $1.114/-0.766 \text{ e} \cdot \text{\AA}^{-3}$ ; goodness-of-fit (on  $F^2$ ) = 1.086. Crystal size:  $0.37 \times 0.30 \times 0.26 \text{ mm}^3$ . All non-hydrogen atoms were refined anisotropically. Hydrogen atoms were included as described for **1**.

## Acknowledgments

This research was supported by the National Science Foundation. The CCD area detector system was purchased in part in 1995 with a NSF Grant (CHE-9310428). Color drawings were prepared with Crystal Maker, Interactive Crystallography. David C. Palmer (P.O. Box 183 Bicester, Oxfordshire, UK OXG TBS).

## References

- [1] (a) L. Manojlovic-Muir, K.W. Muir, B.R. Lloyd, R.J. Puddephatt, *J. Chem. Soc., Chem. Commun.* (1985) 536;  
(b) P.D. Harvey, R. Provencher, J. Gagnon, T. Zhang, D. Fortin, K. Hierso, M. Drouin, S.M. Socol, *Can. J. Chem.* 74 (1996) 2268;  
(c) B.R. Lloyd, L. Manojlovic-Muir, K.W. Muir, R.J. Puddephatt, *Organometallics* 12 (1993) 1231;  
(d) A.L. Balch, B.J. Davis, M.M. Olmstead, *Inorg. Chem.* 32 (1993) 3937;  
(e) T. Zhang, M. Drouin, P.D. Harvey, *J. Chem. Soc., Chem. Commun.* (1996) 877;  
(f) K. Sugimoto, T. Kuroda-Sowa, S.-G. Yan, M. Maekawa, M. Munakata, *Acta Crystallogr., Sect. C* 56 (2000) 414.
- [2] R.J. Puddephatt, L. Manojlovic-Muir, K.W. Muir, *Polyhedron* 9 (1990) 2767, and references therein.
- [3] P.D. Harvey, Y. Mugnier, D. Lucas, D. Evrard, F. Lemaitre, A. Vallat, *J. Cluster Sci.* 15 (2004) 63, and references therein.
- [4] R. Vilar, S.E. Lawrence, S. Menzer, D.M.P. Mingos, D.J. Williams, *J. Chem. Soc., Dalton Trans.* (1997) 3305.
- [5] (a) E.G. Mednikov, *Metalloorgan. Khim.* 2 (1989) 317, [*Organomet. Chem. in the USSR* 2 (1989) 148 (Engl. Transl.)];  
(b) E.G. Mednikov, E.A. Grebenshikova, N.K. Eremenko, *Izv. Acad. Nauk SSSR. Ser. Khim.* (1986) 2155, [*Bull. Acad. Sc. USSR, Div. Chem. Sc.* 35 (1986) 1968 (Engl. Transl.)];  
(c) E.G. Mednikov, N.K. Eremenko, Yu.L. Slovokhotov, Yu.T. Struchkov, *Metalloorgan. Khim.* 2 (1989) 1289, [*Organomet. Chem. in the USSR* 2 (1989) 680 (Engl. Transl.)].
- [6] (a) R.D. Feltham, G. Elbaze, R. Ortega, C. Eck, J. Dubrawski, *Inorg. Chem.* 24 (1985) 1503;  
(b) E.G. Mednikov, N.K. Eremenko, Yu.L. Slovokhotov, Yu.T. Struchkov, S.P. Gubin, *Koordin. Khim. (Sov. J. Coord. Chem.)* 13 (1987) 979 (in Russian);  
(c) J. Dubrawski, K.C. Kriege-Simonsen, R.D. Feltham, *J. Am. Chem. Soc.* 102 (1980) 2089;  
(d) E.G. Mednikov, N.K. Eremenko, S.P. Gubin, Yu.L. Slovokhotov, Yu.T. Struchkov, *J. Organomet. Chem.* 239 (1982) 401;  
(e) E.G. Mednikov, N.K. Eremenko, *Izv. Acad. Nauk SSSR. Ser. Khim.* 11 (1982) 2540, [*Bull. Acad. Sc. USSR, Div. Chem. Sc.* 31 (1982) 2240 (Engl. Transl.)].
- [7] (a) W.-W. du Mont, M. Bätcher, S. Pohl, W. Saak, *Angew. Chem. Int. Ed.* 26 (1987) 912;  
(b) S.M. Godfrey, D.G. Kelly, C.A. McAuliffe, A.G. Mackie, R.G. Pritchard, S.M. Watson, *J. Chem. Soc., Chem. Commun.* (1991) 1163;  
(c) N. Bricklebank, S.M. Godfrey, H.P. Lane, C.A. McAuliffe, R.G. Pritchard, J.-M. Moreno, *J. Chem. Soc., Dalton Trans.* (1995) 2421;  
(d) S.M. Godfrey, C.A. McAuliffe, R.G. Pritchard, J.M. Sheffield, *J. Chem. Soc., Dalton Trans.* (1998) 1919.
- [8] (a) F.A. Cotton, P.A. Kibala, *J. Am. Chem. Soc.* 109 (1987) 3308;  
(b) W.I. Cross, S.M. Godfrey, C.A. McAuliffe, R.G. Pritchard, J.M. Sheffield, G.M. Thompson, *J. Chem. Soc., Dalton Trans.* (1999) 2795.
- [9] E.G. Mednikov, L.F. Dahl, *J. Chem. Soc., Dalton Trans.* (2003) 3117.
- [10] S.A. Ivanov, R.V. Nichiporuk, E.G. Mednikov, L.F. Dahl, *J. Chem. Soc., Dalton Trans.* (2002) 4116.
- [11] E.G. Mednikov, Yu.T. Struchkov, Yu.L. Slovokhotov, *J. Organomet. Chem.* 566 (1998) 15.
- [12] M. Kawano, J.W. Bacon, C.F. Campana, B.E. Winger, J.D. Dudeck, S.A. Sirchio, S.L. Scruggs, U. Geiser, L.F. Dahl, *Inorg. Chem.* 40 (2001) 2554.
- [13] (a) E.G. Mednikov, Ph.D. Thesis, Moscow State University, 1983;  
(b) D.M.P. Mingos, C.M. Hill, *Croat. Chim. Acta* 68 (1995) 745.
- [14] (a) E.G. Mednikov, N.K. Eremenko, *Izv. Acad. Nauk SSSR. Ser. Khim.* (1984) 2781, [*Bull. Acad. Sc. USSR, Div. Chem. Sc.* 33 (1984) 2547 (Engl. Transl.)];  
(b) E.G. Mednikov, N.K. Eremenko, G.A. Hivintseva, *Koordin. Khim. (Sov. J. Coord. Chem.)* 13 (1987) 106 (in Russian);  
(c) E.G. Mednikov, N.I. Kanteeva, *Izv. Acad. Nauk. Ser. Khim.* (1995) 167, [*Russ. Chem. Bull.* 44 (1995) 163 (Engl. Transl.)] and references therein.
- [15] (a) S.M. Godfrey, D.G. Kelly, A.G. Mackie, P.P. Mac Rory, C.A. McAuliffe, R.G. Pritchard, S.M. Watson, *J. Chem. Soc., Chem. Commun.* (1991) 1447;  
(b) C.A. McAuliffe, S.M. Godfrey, A.G. Mackie, R.G. Pritchard, *Angew. Chem. Int. Ed.* 31 (1992) 919.
- [16] D.A. Redfield, J.H. Nelson, L.W. Cary, *Inorg. Nucl. Chem. Lett.* 10 (1974) 727, and references therein.
- [17] (a) J.E. Fergusson, P.F. Heveldt, *Inorg. Chim. Acta* 31 (1978) 145;  
(b) J.A. Rahn, M.S. Holt, M. O'Neil-Johnson, J.H. Nelson, *Inorg. Chem.* 27 (1988) 1316.
- [18] (a) A.D. Ryabov, L.G. Kuz'mina, V.A. Polyakov, G.M. Kazanov, E.S. Ryabova, M. Pfeffer, R. van Eldik, *J. Chem. Soc., Dalton Trans.* (1995) 999;  
(b) N.W. Alcock, W.L. Wilson, J.H. Nelson, *Inorg. Chem.* 32 (1993) 3193;  
(c) R. Fränkel, J. Kniczek, W. Ponikvar, H. Nöth, K. Polborn, W.P. Fehlhammer, *Inorg. Chim. Acta* 312 (2001) 23;  
(d) G.W.V. Cave, W. Errington, J.P. Rourke, *Acta Crystallogr., Sect. C* 55 (1999) 320;  
(e) M. Kubota, S. Ohba, Y. Saito, *Acta Crystallogr., Sect. C* 47 (1991) 1727.
- [19] T.G. Appleton, H.C. Clark, L.E. Manzer, *Coord. Chem. Rev.* 10 (1973) 335.
- [20] E.G. Mednikov, N.K. Eremenko, *Izv. Acad. Nauk SSSR. Ser. Khim.* (1981) 2400, [*Bull. Acad. Sc. USSR, Div. Chem. Sc.* 30 (1981) 1980 (Engl. Transl.)].
- [21] J. Chatt, L.M. Venanzi, *J. Chem. Soc. (A)* (1957) 2351.
- [22] G. Sheldrick: all crystallographic software and sources of the scattering factors are contained in the *SHELXTL* (version 5.1) program library, Bruker Analytical X-ray Systems, Madison, WI.